Aus der Medizinischen Klinik mit Schwerpunkt Rheumatologie und
Klinische Immunologie
der Medizinischen Fakultät Charité – Universitätsmedizin Berlin

DISSERTATION

Immunometabolism of inflamm-aging in naive and memory CD4$^+$ T cells

zur Erlangung des akademischen Grades
Doctor medicinae (Dr. med.)

vorgelegt der Medizinischen Fakultät
Charité – Universitätsmedizin Berlin

von

Yuling Chen
aus Fuzhou, V.R. China

Datum der Promotion: 13.12.2019

Contents

List of Figures

List of Tables

List of Abbreviations

2-DG	2-deoxyglucose
α-Ket	α-ketoglutarate
μg	microgram
AA	antimycin A
AAs	amino acids
AD	Alzheimer's disease
AMD	age-related macular degeneration
AMPK	AMP-activated protein kinase
APC	allophycocyanin
APCs	antigen-presenting cells
ATM	ataxia telangiectasia mutated
ATP	adenosine triphosphate
BCR	B cell receptor
BFA	brefeldin A
BMI	body mass index
BSA	bovine serum albumin
CCF	CO_2 contribution factor
CD	cluster of differentiation
CFDA-SE	5, 6-carboxyfluorescein diacetate succinimidyl ester
CFSE	carboxyfluorescein succinimidyl ester
CMV	cytomegalo virus
CNS	central nervous system
CO_2	carbon dioxide
Con A	concanavalin A
CPT1	carnitine palmitoyl transferase 1
CTLs	cytotoxic T lymphocytes
CXCL10	C-X-C motif chemokine 10

Cy	cyanine
DC	dendritic cell
DMSO	dimethyl sulfoxide
DNA	deoxyribonucleic acid
DNA-PK	DNA-dependent protein kinase
DRFZ	German Rheumatism Research Centre
DUSP	dual-specific phosphatase
EAE	experimental autoimmune encephalomyelitis
ECAR	extracellular acidification rate
EDTA	ethylenediaminetetraacetic acid
ETC	electron transport chain
FA	fatty acid
FABP	fatty acid binding proteins
FACS	fluorescence-activated cell sorting
FADH	flavin adenine dinucleotide
FAO	fatty acid β-oxidation
FAS	FA synthesis
FITC	fluorescein isothiocyanate
FCCP	carbonyl cyanide-p-trifluoromethoxyphenylhydrazone
FSC	forward scatter
G6PD	glucose-6-phosphate dehydrogenase
GAPDH	glyceraldehyde-3-phosphate dehydrogenase
gMFI	geometric mean fluorescence intensity
GLUT	glucose transporter
HEPES	2-[(4-(2-hydroxyethyl)-1-piperazine]ethanesulfonic acid
IU	international Units
IgA	immunoglobulin A
IgD	immunoglobulin D
IgE	immunoglobulin E

IgG	immunoglobulin G
IgM	immunoglobulin M
IFN	interferon
IL	interleukin
IP-10	interferon γ-induced protein 10 kDa
LAL	lysosomal acid lipase
LS	large size
MACS	magnetically-activated cell sorting
MCP-1	monocyte chemoattractant protein-1
mg	milligram
MHC	major histocompatibility complexes
mio	million
ml	milliliter
NADH	nicotinamide adenine dinucleotide
NADPH	nicotinamide adenine dinucleotide phosphate
ng	nanogram
NLR	NOD-like receptors
NK	natural killer
NTs	nucleotides
OCR	oxygen consumption rate
OxPhos	oxidative phosphorylation
PBMC	peripheral blood mononuclear cells
PBS	phosphate-buffered saline
PE	phycoerythrin
PER	proton efflux rate
PerCP	peridinin-chlorophyll-protein
PFKFB3	6-phosphofructo-2-kinase /fructose-2,6- bisphosphatase 3
PMA	phorbol 12-myristate 13-acetate
PMT	photomultiplier tubes

PPMPs	pathogen-associated molecular patterns
PPP	pentose phosphate pathway
PRRs	pattern recognition receptors
RA	rheumatoid arthritis
RLR	RIG-like receptors
RNA	ribonucleic acid
ROS	reactive oxygen species
Rot	rotenone
RPMI	Roswell Park Memorial Institute medium
SSC	sideward scatter
TAG	triacylglycerol
TCA cycle	tricarboxylic acid cycle
TCM	T central memory
TCR	T cells receptor
TEM	T effector memory
Tfh	T follicular helper
Th	helper cells
TLR	toll-like receptors
TNF	tumor necrosis factor
Treg	regulatory T cell
TRM	tissue-resident memory T cell

Abstract

Introduction:

Cellular metabolism modulates effector functions in T cells by providing energy and building blocks. Currently, the metabolic phenotype of human naive and memory $CD4^+$ T cells and how metabolism affects inflamm-aging are not well understood.

Materials and methods:

Naive and memory $CD4^+$ T cells were isolated from young and aged donors (25.0 ± 3.4 years and 57.8 ± 5.7 years). Purity of cells was assessed by flow cytometry. *Ex vivo* naive and memory $CD4^+$ T cells were analyzed in regard to metabolic differences using Seahorse™ Technology to determine proton efflux rate (PER) and oxygen consumption rate (OCR). Proliferation of memory $CD4^+$ T cells was determined by flow cytometry after cell staining with CSFE, and by the expression of Ki-67. Intracellular cytokine expression and cytokine secretion were measured by flow cytometry and multiplex ELISA.

Results:

Memory $CD4^+$ T cells demonstrated a higher basal glycolysis, compensatory glycolysis, as well as basal OCR and spare respiratory capacity than naive $CD4^+$ T cells did. Memory $CD4^+$ T cells from aged donors had lower basal glycolysis and compensatory glycolysis than young donors did, but a higher ratio of basal mitoOCR/glycoPER. Aging had no apparent effect on the cell division proliferation determined by CSFE and Ki-67 in memory $CD4^+$ T cells. Although we did not observe any differences in intracellular cytokine expression, we determined a significantly higher amount of secreted IL-6, IL-9, IP-10, and MCAF in the supernatants of memory $CD4^+$ T cells taken from aged donors than we did using those from young donors.

Summary/conclusions:

Here, we demonstrate a higher basal glycolysis, basal OCR, mitochondrial and glycolytic capacity of human *ex vivo* memory $CD4^+$ T cells than that found in naive T cells. A decrease of basal glycolysis and compensatory glycolysis in memory $CD4^+$ T cells of aged persons which results in an enhanced expression of proinflammatory cytokines and chemokines can be assumed to culminate in T cell dysfunction leading to the

development of inflamm-aging.

Zusammenfassung

Einführung:

Der zelluläre Stoffwechsel moduliert die Effektorfunktionen von humanen T-Zellen, indem er Energie und Bausteine für diese Prozesse liefert. Derzeit ist der metabolische Phänotyp von humanen naiven $CD4^+$ T-Zellen und $CD4^+$ T-Gedächtnis-Zellen des peripheren Blutes und die Auswirkungen des zugrundeliegenden Immunmetabolismus auf „Inflamm-aging“ nicht ausreichend untersucht und verstanden.

Materialen und Methoden:

Naive $CD4^+$ T-Zellen und $CD4^+$ T-Gedächtnis-Zellen wurden aus dem peripheren Blut von jungen und alten Spendern isoliert (25.0 ± 3.4 Jahre und 57.8 ± 5.7 Jahre). Die Reinheit der Zellpopulationen wurde mittels Durchflusszytometrie bestätigt. Um sowohl Glykolyse als auch die mitochondriale Atmung der Zellen zu untersuchen, wurden die Protonen-Efflux-Rate (PER) und die Sauerstoffverbrauchsrate (OCR) von *ex vivo* naive $CD4^+$ T-Zellen und $CD4^+$ T-Gedächtnis-Zellen mittels Seahorse^{TM}-Technologie analysiert. Die mitogen-stimulierte Proliferation von $CD4^+$ T-Gedächtnis-Zellen wurde anhand der CSFE-und Ki-67-Färbung durchflusszytometrisch bestimmt. Die mitogen-stimulierte intrazelluläre Zytokinexpression und Zytokinsekretion wurden mittels Durchflusszytometrie und Multiplex-Elisa gemessen.

Ergebnisse:

$CD4^+$ T-Gedächtnis-Zellen wiesen eine höhere basale Glykolyse, kompensatorische Glykolyse sowie basale OCR und freie Atemkapazität auf als naive $CD4^+$ T-Zellen. $CD4^+$ T-Zellen von älteren Spendern hatten eine niedrigere basale Glykolyse und kompensatorische Glykolyse als junge Spender, jedoch ein höheres Verhältnis von mitoOCR/GlycoPER. Die Proliferationsrate von $CD4^+$ T-Gedächtnis-Zellen wies keine signifikanten altersabhängigen Unterschiede der beiden Spendergruppen auf. Obwohl keine Unterschiede in der intrazellulären Zytokinexpression festgestellt werden konnte, wiesen die Überstände von mitogen-stimulierten $CD4^+$ T-Gedächtnis-Zellen von alten Spendern eine signifikant höhere Menge an sezerniertem IL-6, IL-9, IP-10 und MCAF auf

als die Überstände von mitogen-stimulierten $CD4^+$ T-Gedächtnis-Zellen junger Spender.

Zusammenfassung/Schlussfolgerungen:

Hier zeigen wir eine höhere basale Glykolyse, eine basale OCR, eine mitochondriale und glykolytische Kapazität menschlicher ex-vivo Gedächtnis-$CD4^+$-T-Zellen als naive T-Zellen. Eine Abnahme der basalen Glykolyse, kompensatorische Glykolyse im Gedächtnis $CD4^+$ T-Zellen älterer Menschen, die zu einer verstärkten Expression proinflammatorischer Cytokine und Chemokine führt, kann vermutlich zu einer T-Zell-Dysfunktion führen, die zur Entstehung von altersbedingter chronischer Entzündung führt.

1. Introduction

1.1. Immune system

A sophisticated system known as the immune system has evolved in mammals (including humans) in order to protect the host against foreign pathogens and neoplastic transformed cells. This human defense system is an intricate system and comprises many organs (e.g. bone marrow, thymus, spleen, and lymph nodes), cells (e.g. neutrophils, macrophages, T and B lymphocytes) as well as individual molecules (e.g. immunoglobulins, complement system, cytokines, chemokines and growth factors), all having various characteristics and specialized functions. The main function of the immune system is to distinguish “self” from “non-self” antigens and to maintain the host’s homeostasis. On the one hand, the system eliminates exogenous infections of pathogenic microorganisms such as viruses, bacteria, fungi, parasites and their secretory products, as well as neoplastic transformed cells, dead cells and other damaged components by themselves; on the other hand, it treats damaged organs and tissues to maintain their functions. Generally, the immune system provides two immune strategies: innate and adaptive immunity.

1.1.1. Innate immune system

The innate immune system is usually characterized as an early detection and early protection against infection. The first line of the innate immune system involves physical barriers and chemical barriers[1]. Physical barriers include integral keratinized surface skins and mucosae of the body cavities such as nose, throat, airways, lungs, stomach, intestines, and bladder. Pathogens also need to compete with commensal bacteria in the digestive and reproductive tracts, and overcome chemical barriers including enzymes in saliva, tears, mucus and the low pH values in sweat and gastric acid before reaching the next immune defensive line. In addition to the natural physical and chemical barrier, innate immune system also includes cellular and humoral components. Innate immune cells

comprise professional phagocytes such as macrophages and neutrophils, innate lymphoid cells including natural killer (NK) cells, and professional antigen-presenting cells (APCs) such as dendritic cells which present antigens to T cells of the adaptive immune system[2, 3]. Humoral components of innate immunity include acute phase proteins, complement system, lysozymes, bactericidal permeability increasing factor, antimicrobial peptides, cytokines (IFN, etc.) lactoferrins, and products of the radical metabolism[3].

The innate immune system is a phylogenetically conserved non-specific defense line that targets on pathogen-associated molecular patterns (PPMPs) by pattern recognition receptors (PRRs) such as toll-like receptors (TLR), NOD-like receptors (NLR), and RIG-like receptors (RLR). PPMPs include bacterial lipopolysaccharide, bacterial deoxyribonucleic acid (DNA), mannans, peptidoglycan, lipoteichoic acids, double-stranded ribonucleic acid (dsRNA), and glucans. These PPMPs are highly conserved, commonly observed, and characteristic structures of microbes, but usually not common to the hosts' antigens[4].

1.1.2. Adaptive immune system

The innate immune system recognizes relatively few antigens (most of which are unspecific) while the adaptive immune system mediates its response via antigen-specific receptors, and these specifically detect vast amounts of antigens such as proteins, carbohydrates, lipids and nucleic acids. Furthermore, the adaptive immune system has the ability to establish a "memory" to previously encountered antigens, and this supports a highly rapid-recall response towards the same antigen[5]. The adaptive immune system consists of two major cell types – B and T cells – which are distinguished according to their specific molecules on the cell surface. They convey cellular but also humoral immune response, including immunoglobulins by B cells and cytokines by B and T cells. B and T cells are both derived from hematopoietic stem cells in bone marrow, but they mature in different organs. The antigen-independent maturation process of B cells occurs mainly in the bone marrow before emigrating into the peripheral circulation[6]; but some B cells also mature in the spleen[7], whereas T cells undergo maturation phases in the

thymus[8]. After maturation in primary lymphoid organs (bone marrow/spleen and thymus), B and T cells travel throughout the body searching for dead and abnormal cells, pathogens and invading organisms. The adaptive immune response is triggered in secondary lymphoid organs or peripheral lymphoid organs such as lymph nodes, the spleen, liver, tonsils, and mucosa-associated diffuse lymphoid tissues.

There are five types of immunoglobulins, and these are of the type IgG, IgA, IgM, IgD, and IgE. These immunoglobulins can either act as circulating antibodies or they can be anchored to B-cell membranes. The latter of these are termed the B-cell receptors (BCRs). When BCRs recognizes antigens, B cells undergo “clonal selection” leading to rapid proliferation and differentiation[9]. In the germinal centers of secondary lymphoid organs, activated B cells can then either differentiate to antibody-secreting plasma cells or memory B cells[10]. BCRs are able to recognize antigens directly, whereas T cell receptors (TCR) only recognize short peptides of protein-antigens presented by major histocompatibility complexes (MHC) on the surface of APCs[9].

T cells which express the special surface marker "cluster of differentiation 3" (CD3), undergo positive and negative selection process by interacting with MHC-I and MHC-II complexes in the thymus before maturation. The matured T cells are composed of two subsets: $CD4^+$ and $CD8^+$ T cell defined by surface markers CD4 and CD8, respectively[9]. The matured T cells leave the thymus and enter the circulation in the naive state, and reside quiescently until they encounter any antigens in the vicinity. CD4 and CD8 molecules are part of the TCR complex. CD4 facilitates TCR recognition of antigens presented by MHC-II, while CD8 facilitates TCR-antigen-recognition presented by MHC-I molecular. In the secondary lymphoid organs, $CD8^+$ T cells mature to cytotoxic T lymphocytes (CTLs) which are capable of inducing cytolysis of infected and transformed cells mediated through the FAS pathway or by granzyme and perforin-mediated cell lysis. Furthermore, CTLs produce cytokines, such as TNF and IFN-γ, in order to carry out their cytotoxic action[11].

Naive $CD4^+$ T cells differentiate into effector T-cell lineages with unique characters, but different functions. These include T helper cells type 1 (Th1 cells), Th2 cells, Th9 cells,

Th17 cells, and T follicular helper (Tfh) cells, as well as regulatory T cells (Treg cells). Treg cells can be also generated in the thymus.

After primary responses, the majority of effector T cells do not achieve survival, but a small population of effector T cells do survive to become long-lived memory cells[12]. The CD45 molecule is a tyrosine phosphatase that modulates cellular stimulation. The expression of CD45 isoforms on the cell surface can be used to distinguish naive from memory T cells. In humans, naive T cells from the peripheral blood are defined as CD45RA-positive CD45RO-negative, whereas memory T cells from the peripheral blood are defined as CD45RA-negative and CD45RO-positive[13].

1.2. Aging

The aging population of Europe is expanding because of the increase in life expectancy and low birth rates. The old-age dependency ratio (the ratio of persons aged 65 years and above to those aged 15-64 years) will reach 53.5% by 2060[14]. Physiological aging of aged people is a biological phenomenon but results in increasing health problems such as cancer, Alzheimer's disease (AD), type 2 diabetes mellitus, stroke, and cardiovascular diseases[15, 16].

1.2.1. Inflamm-aging

There are seven pillars which have been noted to contribute to aging and aging-related diseases: inflammation, adaption to stress, epigenetics, macromolecular damage, metabolism, proteostasis, and finally stem cells and regeneration[17]. More importantly, these seven pillars do not affect aging and aging-related diseases independently from each other; actually they are rather highly interconnected and, mutually influential[17].

Damage of any closely connected aging pillars results in inflammation which is the hub of aging, and this has been termed "inflamm-aging"[18, 19]. On the one hand, inflamm-aging indicates a chronic, sterile, low-grade inflammatory status, on the other hand it is a decline in the ability of eliminating a variety of antigens[19]. Inflamm-aging is characterized by an

elevation of the levels of IL-6, TNF, and IL-1 which participate in the pathogenesis of most age-related diseases and are strong predictors of morbidity and mortality during aging[20]. Macrophages – one type of cells connected with the innate immune response – play a crucially important role in the process of inflamm-aging. For example, one of their main targets is chronic antigen stress. Macrophages are not the only cells related to the process of inflamm-aging. In addition, other cells such as neutrophils, dendritic cells, and NK cells of the innate immune response are able to produce pro-inflammatory mediators an thus are also essential parts of the process of inflamm-aging[20].

Although the innate immune system plays an important role in inflamm-aging, the adaptive immune system also participates to a high degree in inflamm-aging[19]. Moreover, as the innate immune system impacts the adaptive immune system in many ways, changes in the innate immune system within aging also have an effect on the response of the adaptive immune system[21, 22, 23, 24, 25]. Decreased proliferative capability of $CD4^+$ T cells in elderly persons is associated with a faster loss of activation-related antigens and accumulation of regulatory T cells.

Inflamm-aging is derived from immunosenescence[19]. Immunosenescence is more related to the adaptive immune system. Immunosenescence is defined a functional decline in immune system that occurs with aging. The change in cell populations can be measured by immune parameters, and is related to the increased susceptibility of aged people to infection, inflammatory age-related diseases and also their decreased response to vaccination[18, 26].

1.2.2. Age-related changes in the adaptive immune system

With increasing age, changes in the B cell compartment occur, and these include (i) reduced B cell maturation in the bone marrow, (ii) an increase in peripheral memory B cells, (iii) a decrease in peripheral naive B cells, and (iv) a decline in the response ability to stimulatory molecules, and hampered response ability to vaccination[20].

As for T cells, the absolute numbers and percentages of human $CD8^+$ naive T cell compartment decreases in peripheral blood during aging[27, 28]. $CD8^+$ T cell alterations with

increased aging also involves an increase of effector memory T cells in cytomegalo virus (CMV) positive humans[28] and decreased diversity of TCR repertoire, and a largely increased T cell clonality[29].

In contrast to $CD8^+$ naive T cells, the naive $CD4^+$ T cell compartment maintains their cell numbers during aging[28]. Maintenance of peripheral naive $CD4^+$ T cell pool in adults is independent of thymic output, which peaks at puberty and declines dramatically thereafter, but is still maintained by the existing peripheral T cell pool[30]. Similar to the human $CD8^+$ naive T compartment, the TCR repertoire diversity of naive $CD4^+$ T cells contracts two to five-fold during aging[29]. In addition, the $CD8^+$ naive T cell compartment demonstrates higher age-related increase in clonality, when compared to the naive CD4 compartment. The decrease in naive T cell compartment parallels with the increase in different subsets of memory T cells due to the accumulation of TCR-engaging events during aging[31]. Virtual memory T cells develop from naive cells but without encountering antigens[32]. During aging, a fraction of the $CD8^+$ or $CD4^+$ naive T cells gather a memory-like phenotype. This is namely one of virtual memory, and thus those cells are then impaired in their ability to expand. Continuous infections, most commonly those caused by CMV, result in the accumulation of end-differentiated memory T cells, and these are known as senescent T cells. These cells have senescent-specific surface marker expression including that of CD27−CD28−CD57+KLRG−1+ and probably also short telomeres, leading to a decline in the ability of proliferation[26, 31]. In the CD4 T cell compartment, senescent memory cells which re-expressed CD45RA have a poorer vaccine response[34] and prefer to infiltrate tissue and cause tissue damage due to higher levels of granzyme B and perforin expression[35]. These senescent T cells also express high amounts of inflammatory cytokines such as IFN-γ and TNF-α after activation. This is called the senescence-associated secretory phenotype (SASP) which evolves in the course of inflamm-aging[36]. Besides well-known aging related diseases, inflammatory environment due to senescent T cells also contributes to autoimmune diseases, such as RA, ANCA-associated vasculitides and systemic lupus erythematosus[37]. Aging influences components of $CD4^+$ T cell subsets. The accumulation of FOXP3(+) Tregs is a link to chronic Infections because their spontaneous reactivation has suppressed the production of IFN-γ during

aging[38]. The ratio of Treg/Teff increases and thus results in poorer responses to influenza vaccination[39].

1.3. Glycolysis and the tricarboxylic acid cycle (TCA cycle)

Cells follow two major pathways of producing ATP to meet cellular bioenergetics demands: (i) glycolysis, and (ii) the tricarboxylic acid cycle (TCA cycle) which is linked with oxidative phosphorylation (OxPhos). Glycolysis begins with an uptake of extracellular glucose from the surrounding environment by glucose transporters (GLUTs). Glycolysis undergoes a series of metabolic reactions which leads to the breakdown of one molecule of glucose containing six carbon atoms to two molecules of pyruvate which each contain three carbon atoms. In the process of glycolysis, every molecule of glucose only generates two molecules of ATP which is in bioenergetics (regarding cellular ATP production) termed a low-efficient pathway. But more importantly, glycolysis generates intermediates for the synthesis of nucleotides, amino acids and lipids to support cell growth, differentiation, proliferation and production of effector molecules such as cytokines, chemokines and adhesion molecules[40, 41, 42, 43]. Finally, pyruvate is either metabolized to lactate which is then secreted to the external matrix, or directly transferred to mitochondria and catabolized to acetyl-CoA for fueling the TCA cycle. TCA cycle enzymes are located in the mitochondrial matrix. Of note, the TCA cycle itself is a critical link in all cellular metabolic pathways: Acetyl-CoA produced by fatty acid (FA) β-oxidation (FAO) joins in to the TCA cycle via being metabolized to citrate, and glutamine fuels the TCA cycle via glutaminolysis to α-ketoglutarate (α-Ket). The TCA cycle generates reduced nicotinamide adenine dinucleotide (NADH) and flavin adenine dinucleotide ($FADH_2$), which both transfer electrons into complexes I and II of the electron transport chain (ETC). As a result of electron transport, the mitochondrial proton gradient is generated by pumping protons to the outer side of the mitochondrial membrane which is then used for OxPhos by driving the ATP synthase to efficiently generate 36 molecules of ATP, all out of one molecule of glucose.

Under anaerobic conditions, pyruvate is mainly reduced to lactate instead of fueling the TCA cycle. Activated lymphocytes highly rely on glycolysis only as long as the oxygen supply is sufficient. The process of aerobic glycolysis which was firstly observed by Otto Warburg is now also termed the Warburg effect[40, 41, 44, 45].

1.3.1. T cell metabolism

Naive $CD4^+$ T cells as well as memory $CD4^+$ T cells are relatively long-lived, quiescent immune cells which travel throughout the body and do not differentiate, grow or expand. They produce immunomodulatory molecules only until they encounter cogent antigens presented by professional APCs. They have very few biosynthetic needs other than some housekeeping functions, for which ATP alone – mainly generated by OxPhos – is sufficient for maintaining cellular demands[42, 46]. Naive T cells use up to three sources for the generation of mitochondrial ATP:

1. glucose-derived pyruvate,
2. glutamine-derived α-Ket,
3. FAO-derived acetyl-CoA[46, 47, 48].

When encountering antigens, T cells are activated and quickly undergo proliferation, differentiation and the production of great amounts of immunomodulatory molecules in order to reduce the amount of antigens[41, 49, 50]. To fulfil the demand of moderately increased ATP amounts and the multitude of biosynthetic intermediates in the activated state[43, 46], T cells increase the metabolite flux through TCA cycle and OxPhos, a feat which is accompanied by a speeding up of the rate of glycolysis[51, 52, 53].

However, subsequent to antigen clearance, a small part of the effector T cells remains vital, survives and becomes memory T cells. These cells have the ability to induce mitochondrial biogenesis which finally ensures the energy generation through OxPhos[54]. Memory and naive T lymphocytes primarily use the TCA cycle and OxPhos to maintain survival, but memory T cells prefer fueling the mitochondrial TCA cycle with FAO.

1.3.2. Metabolism in T cells during aging

Only very few studies have addressed the metabolic phenotype in immune cells during aging. There are some clues that aging or senescence in T cells affects their metabolism. One study performed on human CD45RA positive $CD8^+$ memory T cells (so-called $CD8^+$ TEMRA cells) revealed that these cells are defective in mitochondrial biogenesis and mitochondrial function leading to a low OCR/ECAR ratio and low spare respiratory capacity (SRC). These $CD8^+$ TEMRA cells demonstrate a metabolic profile which relies mainly on glycolysis for energy production while enhancing the expression of both TNF-α and IFN -γ[55]. Interestingly, inhibition of p38 MAPK signaling in senescent $CD8^+$T cells recovered mitochondrial biogenesis and reversed their senescent phenotype which was mTORC1-independent, but it did not change glucose uptake or oxidative phosphorylation. The energy sensor AMP-activated protein kinase (AMPK) is activated in energy-deprived T cells. Memory $CD4^+$ T cells in persons older than 65 years showed an overexpression of the dual-specific phosphatase 4 (DUSP4) which is a downstream target molecule of activated AMPK[56]. Increased DUSP4 expression of activated T cells in the elderly results in an impaired ability of support B-cell differentiation leading to defective adaptive immune responses[56].

However, the metabolic phenotype of human naive and memory $CD4^+$ T cells and how metabolism affects functions of naive and memory $CD4^+$ T cells during aging still remains not well understood.

1.4. Objectives

Here, we hypothesize that metabolic change in human $CD4^+$ T cells during aging may result in T cell dysfunction leading to the development of aging-related diseases. First, we investigated the metabolic phenotype of human naive and memory $CD4^+$ T cells. Secondly, we aimed to clarify the metabolic differences in naive and memory $CD4^+$ T cells between young and aged donors. Finally, we addressed the specific function (such as cytokine expression and proliferation ability) of these cells.

2. Materials and methods

2.1. Materials

2.1.1. Media

Table 2-1: Cell culture media and supplements

Product	Company	Catalog number
RPMI 1640 medium GlutaMAX™ Supplement*	Thermo Fisher Scientific	61870-010
Seahorse XF RPMI Medium (without phenol red)**	Agilent	103336-100

*The media were mixed with 5% human AB serum and 1% (w/v) penicillin/streptomycin.

** The media were mixed with 10 mM D-glucose, 1 mM pyruvate, 2 mM glutamine and 1 mM HEPES.

2.1.2. Antibodies

Table 2-2: Antibodies

Antigen	Conjugated with	Company	Clone	Catalog number	Isotype	Dilution
hCD3	Pacific Blue	BD Biosciences	UCHT1	558117	mouse IgG1, κ	1:50
hCD4	FITC	DRFZ	TT1	-	mouse IgG1	1:1600
hCD45RO	PE	DRFZ	UCHL1	-	mouse IgG2a, κ	1:100
hCD45RA	APC	DRFZ	4G11	-	mouse IgG2a	1:400
hINFγ	Percp-Cy5.5	Biolegend	4S.B3	502526	mouse IgG1, κ	1:100
hIL-2	APC-vio770	Miltenyi Biotec	N7.48 A	130-097-011	mouse IgG2a, κ	1:10
hIL-4	PE	Miltenyi Biotec	7A3-3	130-091-647	mouse IgG1, κ	1:10
hIL-17A	FITC	Miltenyi Biotec	CZ8-23G1	130-094-520	mouse IgG1, κ	1:10
hKi-67	PerCP-Vio700	Miltenyi Biotec	REA183	130-100-292	recombinant human IgG1	1:11
hTNF-α	PE-Vio770	Miltenyi Biotec	cA2	130-096-755	human IgG1	1:10

2.1.3. Chemicals and antibiotics

Table 2-3: List of chemicals

Chemical	Company
2-deoxyglucose (2-DG)	Sigma Aldrich
5, 6-carboxyfluorescein diacetate succinimidyl ester (CFDA-SE)	Sigma Aldrich

Chemical	Company
Antimycin A (AA)	Sigma Aldrich
Brefeldin A (BFA)	Sigma Aldrich
Carbonyl cyanide-p-trifluoromethoxyphenylhydrazone (FCCP)	Sigma Aldrich
D-glucose	Sigma Aldrich
Dimethyl sulfoxide (DMSO)	Sigma Aldrich
Ethanol	Carl Roth
Ethylenediaminetetraacetic acid (EDTA)	Sigma Aldrich
Glutamine	Sigma Aldrich
Ficoll-Paque™PLUS	GE Healthcare
Flebogamma	Baxter
2-[(4-(2-hydroxyethyl)-1-piperazine]ethanesulfonic acid (HEPES)	Sigma Aldrich
Human AB Serum	Sigma Aldrich
Ionomycin	Sigma Aldrich
IL-2	PROLEUKIN®
Phorbol 12-myristate 13-acetate (PMA)	Sigma Aldrich
Poly-D-Lysine	Sigma Aldrich
Pyruvate	Sigma Aldrich
Rotenone (Rot)	Sigma Aldrich
Trypan blue solution	Sigma Aldrich

Table 2-4: Antibiotics

Antibiotic	Company
Penicillin/streptomycin	Thermo Fisher Scientific

2.1.4. Solutions and buffers

Table 2-5: Solutions and buffers

Solutions and buffers	Company
Phosphate-buffered saline (PBS)	80 mM Na_2HPO_4, 19 mM $NaH_2PO_4 \cdot 2H_2O$, 100 mM NaCl (pH 7,6)
PBS/BSA	PBS + 1%(w/v) BSA
PBS/BSA/azid	PBS/BSA + 0,05% (w/v) NaN_3
autoMACS® Running Buffer	PBS/BSA + EDTA + 0.09% azide

2.1.5. Kits

Table 2-6: Kits

Kit	Company
CD4 microbeads, human	Miltenyi Biotec
Inside staining kit	Miltenyi Biotec
Naive $CD4^+$cell Isolation Kit II, human	Miltenyi Biotec
Memory $CD4^+$ T Cell Isolation Kit, human	Miltenyi Biotec
T Cell TransAct™, human	Miltenyi Biotec

2.1.6. Devices

Table 2-7: Devices

Devices	Company
Allegra® X-15R Centrifuge	Beckman Coulter
Bio-Plex suspension system	Bio-Rad
CO_2 incubator	Thermo Fisher Scientific
FACS Canto®II	BD Biosciences
Microscope	Hund Wetzlar
Non-CO_2 incubator	Thermo Fisher Scientific
PH meter PH1100	VWR International
Seahorse XFe96 Analyzer	Agilent
Vortex mixer MX-S	DLAB

2.1.7. Miscellaneous materials

Table 2-8: Miscellaneous materials

Material	Company
0.2 µM Sterilfilter	SARSTEDT
0.5, 1.5, and 2 ml reaction tubes	SARSTEDT
0.2 µm filter	SARSTEDT
6-,12-,24-,48-, and 96-well plates	Greiner Bio-One
5 ml polystyrene tubes	SARSTEDT
10 ml, 25 ml pipettes	SARSTEDT
15 ml, 50 ml polypropylene-tube	SARSTEDT
25 ml pipettes	SARSTEDT
25 ml syringes	BD Biosciences
LS MACS™ columns	Miltenyi Biotec
MACS™ Separator	Miltenyi Biotec
MACS™ MultiStand	Miltenyi Biotec
Counting chamber	Paul Marienfeld

Seahorse XF Calibrant Solution	Agilent
Seahorse XF96 Cell Culture Microplates	Agilent
Seahorse XF96 Extracellular Flux Assay Kit	Agilent
Steritop™ filter units	Merck Millipore

2.1.8. Software

Table 2-9: Software

Software	Company
EndNote x7	Thomson Reuters
FACS®Diva	BD Biosciences
FlowJo 7.2.5 and V10	Tree Star.
GraphPad® Prism Version 6.0	GraphPad Software
Microsoft® Office 365 ProPlus	Microsoft
Seahorse Wave Version 2.6.0	Agilent

2.2. Methods

2.2.1. Cell purification

2.2.1.1. Peripheral blood mononuclear cells (PBMCs) preparation

Filters from young donors (<35 years) and aged donors (>50 years), whose personal information is pseudonymized for the researchers, were provided by the Charité blood donation department. PBMCs were purified by density gradient separation using Ficoll-Paque™PLUS (GE Healthcare) as a separation solution. The principle of this method is that different cell types form their own cell layers during the centrifugation, according to their different densities. The density of Ficoll is 1.077 g/l at room temperature, which is lower than red blood cells and granulocytes, but higher than the density of PBMCs and platelets. The latter are therefore separated onto the surface of ficoll after gradient centrifugation. First, cells were flushed out of the filter using a syringe (BD Biosciences) filled with autoMACS® Running Buffer (Miltenyi Biotec) up to a total volume of 140 ml; the resulting diluted cell suspension was well mixed and then distributed into four 50-ml tubes. 35 ml of diluted cell suspension was layered carefully onto the surface of 15 ml of Ficoll-

Paque^{TM}PLUS by pipetting slowly down along the 50-ml tube (SARSTEDT) tube wall using a 25-ml pipette (SARSTEDT); then the tubes were centrifuged at 400×g, at 20 °C for 35 minutes without breaks. The PBMC-containing white layer was collected into two 50-ml tubes, washed 2 twice by increasing the volume up to 50 ml with autoMACS® Running Buffer, and centrifuging at 300×g and 4 °C for 10 min. Finally, the supernatant was aspirated completely.

2.2.1.2. Naive/memory CD4$^+$ T cell purification

CD4$^+$ naive/memory T cells were isolated from PBMCs by application of the magnetically activated cell sorting (MACS) device according to modified manufacturer's instructions which consist of microbeads-labeled cell depletion by the naive CD4$^+$ cell Isolation Kit II (Miltenyi Biotec) and Memory CD4 T Cell Isolation Kit, human (Miltenyi Biotec) which were followed by a positive selection of microbeads-labeled cells using CD4 microbeads (Miltenyi Biotec). In short, PBMCs were labeled by naive/memory CD4$^+$ T cell-biotin-conjugated antibodies, and after incubation at 4 °C, anti-biotin microbeads were added. The microbeads-labeled cell suspension was pipetted onto an LS MACS column (Miltenyi Biotec) placed in the magnetic field of the MACS™ Separator (Miltenyi Biotec), and the unlabeled cells that pass through were collected. Subsequently, isolated unlabeled CD4$^+$ naive/memory T cells were incubated for 5 min in ice with 5 mg/ml of flebogamma (Baxter) to block Fc receptors. This was followed by adding CD4 magnetic beads and incubating for 15 min at 4 °C, and then washed by adding autoMACS® Running Buffer (Miltenyi Biotec). Labeled cells were resuspended in autoMACS® Running Buffer and applied onto an LS MACS column (Miltenyi Biotec). After washing the column 3 times with autoMACS® Running Buffer, labeled cells were flushed out of the column by pushing the plunger. The purity of naive CD4$^+$T cells (CD3+CD4+CD45RO-CD45RA+) and memory T cells (CD3+CD4+CD45RO-CD45RA+) was checked by flow cytometry using the following: anti-human-CD3: Pacific Blue (BD Biosciences, clone UCHT1, Cat.# 558117); anti-human-CD4: FITC (DRFZ, clone TT1); anti-human-CD45RO: PE (DRFZ clone UCHL1), and anti-human-CD45RA: APC (DRFZ, clone 4G11).

2.2.2. Cell counting method

Neubauer Chamber: Cell suspensions were mixed (1:1 v/v) with a trypan blue solution (Sigma Aldrich). Trypan blue cannot pass through the intact live cell membrane; only dead and damaged cells with a damaged membrane can be stained with trypan blue. A 10 µl cell / trypan blue mixture was transferred to a Neubauer chamber, after which the cell number was counted in the four squares under the microscope. The cell number in a 1-mm suspension was determined by multiplying the average number taken out of four squares by the number of cells, the dilution factor and the chamber factor (10,000).

2.2.3. Cell stimulation

2.2.3.1. Non-specific cell stimulation for the induction of intracellular cytokine synthesis by PMA and ionomycin

Isolated $CD4^+$ memory T cells were resuspended in RPMI 1640 medium (Thermo Fisher Scientific) with 5% human AB Serum (Sigma Aldrich), and 1% penicillin/streptomycin (Thermo Fisher Scientific), seeded at a concentration of $5x10^6$/ml in a 96-well flat bottom plate (Greiner Bio-One). Phorbol 12-myristate 13-acetate (PMA, Sigma Aldrich) and ionomycin (Sigma Aldrich) were added and incubated at 37 °C under 5% CO_2 in an incubator for 2 hours. Afterwards, brefeldin A (BFA, Sigma Aldrich) was added and incubated for another 3 h. BFA is a lactone antibiotic from *Penicillium brefeldianum*. It specifically inhibits protein traffic by interrupting the function of the Golgi apparatus.
PMA (Sigma Aldrich) was dissolved in dimethyl sulfoxide (DMSO, Sigma Aldrich) as a stock solution of 1 mg/ml, pre-diluted to 1 µg/ml, and then used at a final concentration of 10 ng/ml. Ionomycin was dissolved in DMSO at a stock solution of 1 mg/ml and used at a final concentration of 1 µg/ml. BFA was dissolved in DMSO as a stock solution of 5 mg/ml and used at a final concentration of 2 µg/ml.

2.2.3.2. Specific cell activation for proliferation by anti-human CD3 and CD28

$CD4^+$

memory T cells were resuspended in RPMI 1640 medium (Thermo Fisher Scientific) with 5% human AB Serum, and 1% penicillin/streptomycin (Thermo Fisher Scientific), adjusted to a concentration of $1x10^6$/ml, seeded at 200 µl in every well of a 96-well flat bottom plate (Greiner Bio-One). Cells were stimulated by T Cell TransAct™ (Miltenyi Biotec) supplemented with IL-2 (PROLEUKIN®) at 37 °C under 5% CO_2 in 96-well flat plates.

IL-2 was dissolved in PBS at a stock solution of 18 million International Units (IU)/ml, and later used at a final concentration of 36 IU/ml.

T Cell TransAct™ was used for the activation and expansion of quiescent T cells; basically, it comprises humanized recombinant CD3 and CD28 agonists.

2.2.4. Antibody staining and flow cytometry analysis

2.2.4.1. Surface molecules staining

For surface molecule staining, cells were harvested and washed by phosphate-buffered saline (PBS) supplemented with bovine serum albumin (BSA) and 2 mM ethylenediaminetetraacetic acid (EDTA) (PBS/BSA/EDTA, German Rheumatism Research Centre, DRFZ), and stained for 10 min in the dark at 4 °C with 100 µl of a combination of monoclonal antibodies including anti-human-CD3 (using Pacific Blue, BD Biosciences, clone UCHT1, Cat. # 558117), anti-human-CD4 (FITC, DRFZ, clone TT1), anti-human-CD45RO (PE, DRFZ, clone UCHL1), and anti-human-CD45RA (APC, DRFZ, clone 4G11). Afterwards, cells were washed with 1 ml of PBS/BSA/EDTA in order to remove residual antibodies, and then centrifuged at 300×g for 10 minutes at 4 °C. The supernatant was aspirated, after which the cell pellet was resuspended in PBS/BSA/azide, and stored in ice prior to analysis by flow cytometry.

2.2.4.2. Intracellular cytokine staining

Intracellular cytokine staining was done according to the manufacturer's instructions. Briefly, after PMA-ionomycin stimulation, cells were collected, washed with

PBS/BSA/EDTA (300×g for 10 minutes at 4 °C) after which the, cell pellet was resuspended and fixed with Inside Fix (Inside staining kit, Miltenyi Biotec) for 20 minutes in the dark at room temperature. This was again centrifuged (300×g for 10 minutes at 4 °C) and the supernatant aspirated completely. The cells were then stained for 15 min at room temperature in the dark by adding master mixes of following antibodies: anti-human-INFγ (Percp-Cy5.5, Biolegend, clone 4SB3, Cat.# 502526), anti-human-IL-2 (APC-vio770, Miltenyi Biotec, clone N7.48 A, Cat.# 130-097-011), anti-human-IL-4 (PE, Miltenyi Biotec, clone 7A3-3, Cat.# 130-091-647), anti-human-IL-17A (FITC, Miltenyi Biotec, clone CZ8-23G1, Cat.# 130-094-520), and anti-human-TNF-α (PE-Vio770 (Miltenyi Biotec, clone cA2, Cat.# 130-096-755). Subsequently, cells were washed by adding Inside Perm (Inside staining kit, Miltenyi Biotec) in order to remove residual antibodies, and centrifuged at 300×g and 4 °C for 10 minutes. Supernatants were discarded and cell pellets were resuspended in PBS/BSA/azide, and stored on ice until further analysis by flow cytometry.

2.2.4.3. 5, 6-carboxyfluorescein diacetate succinimidyl ester (CFDA-SE) staining

5, 6-carboxyfluorescein diacetate succinimidyl ester (CFDA-SE, Sigma Aldrich) is a permeable non-fluorescent dye with a succinimidyl ester which can covalently bind to intracellular free amines; acetate groups of CFDA-SE are cleaved by intracellular esterases within viable cells so as to generate membrane-impermeant carboxyfluorescein with a green fluorescence. As carboxyfluorescein succinimidyl ester (CFSE)-labeled cells divide, carboxyfluorescein-labeled molecules are allocated equally to daughter cells, whereby each daughter cell receives nearly half of the fluorescence intensity from its parent cell. Thus, each cell generation can be assessed according to the various amounts of cell fluorescence recorded via flow cytometry. Before activation, cells were labeled with CSFE. In brief, cells prior to stimulation were resuspended up to a concentration of $20x10^6$ /ml in PBS, and then the same volume of CFSE (5 µM) in PBS was added. The final concentration of CFSE was 2.5 µM. After incubation in the dark at room temperature for 5 min, the labeled cells were washed 10 times with culture medium.

CSFE-labeled $CD4^+$ memory T cells were stimulated as described for the previous method. After 72 h and 96 h, the cells were harvested and analyzed by flow cytometry. The evaluation of the proliferation data was analyzed by utilizing FlowJo (Tree Star). The division index (DI), proliferation index (PI) and percentage of divided cells (% divided) are shown below in equations I, II and III (respectively) and were calculated according to the FlowJo manual, where i = division number (undivided = 0), and N(i) = number of events in division (http://docs.flowjo.com/vx/experiment-based-platforms/proliferation/):

(I) $$\text{Division index} = \frac{\sum_{i=1}^{i}(i * N(i)/2^i)}{\sum_{i=0}^{i}(N(i)/2^i)}$$

(II) $$\text{Proliferation index} = \frac{\sum_{i=1}^{i}(i * N(i)/2^i)}{\sum_{i=1}^{i}(N(i)/2^i)}$$

(III) $$\%\ \text{Divided} = \frac{\text{Division index}}{\text{Proliferation index}}$$

The division index is the average number of divisions for the cells in the original starting population. The proliferation index indicates the average number of divisions of dividing cells. The percentage of divided cells reveals the number of cells which have divided at least once.

CFDA-SE was dissolved in DMSO at a stock solution of 5 mM, stored in -20 °C and then used at a final concentration of 2.5 µM.

2.2.4.4. Anti-human-Ki-67 staining

Ki-67 protein expression is detectable during all active phases of the cell cycle [G(1), S, G(2)) and mitosis], but not in the G (0) (phase of quiescent cells). Thus, Ki-67 protein expression corresponds to proliferating cells and serves as a good proliferation marker in order to determine the growth fraction of a given cell population. For Ki-67 staining, cells were stimulated for 72 h or 96 h according to the protocol previously described, harvested and fixed by the addition of 70% ethanol at -20 °C in a refrigerator for at least 1 h, washed twice by adding PBS/BSA, centrifuging at 300×g and 4 °C for 10 minutes, aspirating the supernatant completely, suspending the cells in 100 µl of PBS/BSA, and then adding 10

µl of anti-human-Ki-67 (PerCP-Vio700, Miltenyi Biotec, clone REA183, Cat.# 130-100-292) This was mixed well and incubated for 20 min at room temperature in the dark. Subsequently, 1 ml of PBS/BSA was added, and the mix was centrifuged at 300×g for 10 minutes. After complete aspiration, cells were resuspended in PBS/BSA/azide, and kept on ice until they were subjected to flow cytometry.

2.2.4.5. Flow cytometry

Flow cytometry was originally introduced in the late 1960s. Nowadays it is a well-established cell biology technique for the analysis of physical and chemical properties within various cell populations. In brief, the principle of flow cytometry is as follows: cells' surface proteins or intracellular molecules such as cytokines and transcription factors are labeled with fluorochrome-conjugated antibodies, drawn up and then passed singly though an interrogation point caused by hydrodynamic focusing initiated by an outer sheath fluid. At the interrogation point, electrons of the fluorescent dye are excited and rise to high energy states via an intersecting laser beam, and light is produced when the electrons withdraw to their original low-energy states. The lightings are collected and separated according to the particular wavelengths of different filters, and then detected by photomultiplier tubes (PMT). After the laser beam intersects the cells, light scattering is produced around the edges of the cell, due to diffraction. This light scatter is named as forward scatter (FSC) and collected at a small angle range (less than 10°) relative to the laser beam. In addition, side scatter (SSC) is the laser light reflected off the cell and internal structure and collected at an angle of 90° to the laser beam. FSC correlates with cell size and SSC with granularity or internal complexity.

All stained cells were measured in a BD FACS Canto®II device by use of the FACS®Diva software (BD Biosciences), and analyzed using FlowJo software (Tree Star). Dead cells and debris were excluded from the analysis according to FSC and SSC signals.

2.2.5. Metabolic Assays

Metabolic Assays were performed in an Agilent Seahorse XFe96 analyzer which can detect cellular oxygen concentration and proton concentration on a rapid, easy and real-time manner. Before starting the Seahorse XF assay measurement, the assay cartridge with a utility plate containing the Seahorse XF calibrant is loaded into the Agilent Seahorse XFe96 analyzer in order to allow automatic calibration of biologically compatible optical sensors. Subsequently, the 96-well culture plate is loaded into the instrument. When starting the measurement, sensor probes closer down to the Seahorse XF RPMI Medium (without Phenol Red) create a transient microchamber 200 microns above the cell monolayer. The real-time changes of oxygen and proton levels can be detected sensitively, and precisely in the transient microchamber. Once a measurement is finished, the sensor probes go up and down slowly in order to mix medium restoring extracellular oxygen and proton levels to baseline. Up to four inhibitors, stimulants, substrates, or compounds may be loaded to the assay delivery cartridge ports for automated injection during the measurement. Baseline oxygen consumption rate (OCR) and proton efflux rate (PER) are measured prior to injections. After injection, the sensor probe gentle mixes the medium, and then starts measurement (**Figure 2-1**). The duration of each measurement, mixture and drug delivery can be defined by using the Seahorse Wave software (Agilent).

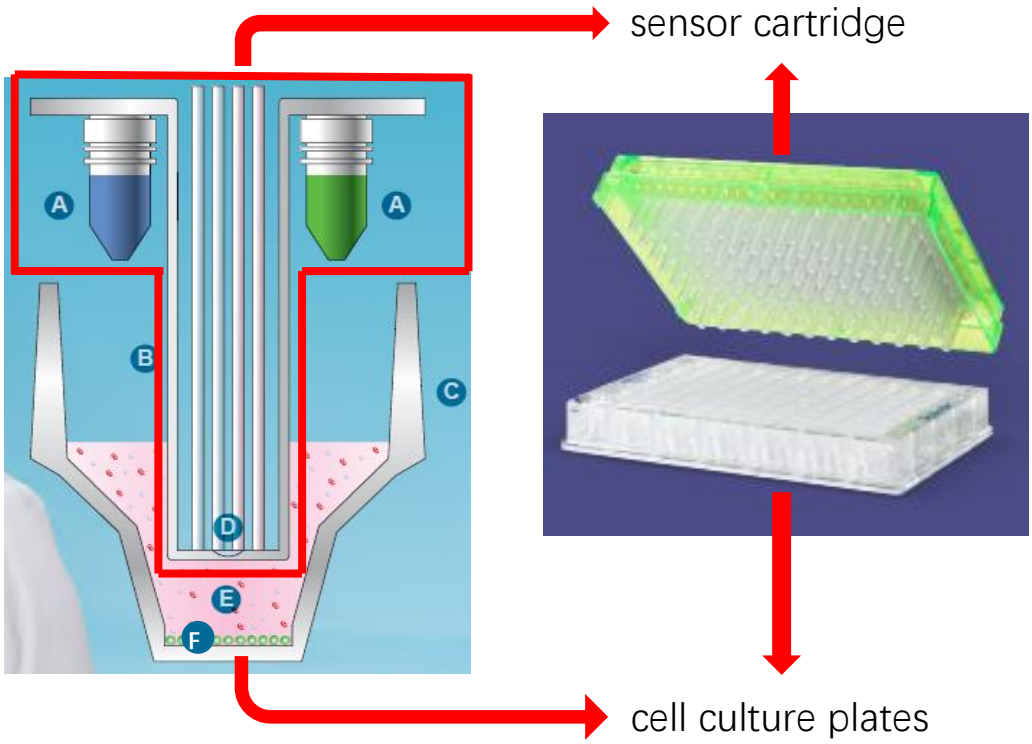

Figure 2-1: Main structures of the Seahhorse sensor cartridge and cell culture plate. (A) Integrated injection port: loaded with up to 4 inhibitors, stimulants, substrates, or compounds injected according to protocol in order to create multiple conditions in each well. (B) Sensor probe: slowly lowered in order to create a transient microchamber where real-time oxygen and proton concentrations can be rapidly measured in the extracellular medium; or gently moved up or down to restore oxygen and proton concentrations to baseline. (C) Cell culture microplate: cell suspension container. (D) Biologically compatible optical microsensors: these include polymer-embedded fluorophores which measure oxygen and proton concentrations without any dye. (E) Transient microchamber: this allows sensitive, precise measurements of oxygen and proton concentrations in real-time. (F) Cell monolayer. (Modified from Agilent.com)

Human naive/memory $CD4^+$ cells were cultured overnight at 37 °C, under 5% CO_2 in an incubator using RPMI 1640 medium supplemented with 5% human AB Serum, and 1% penicillin/streptomycin. One day before analysis, the Agilent Seahorse XFe96 analyzer was turned on in order to warm it up to exactly 37 °C; the experimental setting was adjusted on the Agilent Seahorse XFe96 analyzer; the sensor cartridge was hydrated with sterile water (200 µl/well in the non-CO_2 incubator at 37 °C overnight); 20 ml of Seahorse XF Calibrant (Agilent) was filled into a 50-ml tube and kept in the non-CO_2 incubator at

37 °C overnight; in order to prevent cell movement during measurement, cell culture plates were coated with Poly-D-Lysine (Sigma Aldrich) for 90 min at room temperature, following by 2 washes each with 200 µl of sterile water. Finally, it was left on the bench to dry.

2.2.5.1. Mito Stress Test and Glycolytic Rate Assay

The Mito Stress Test and Glycolytic Rate Assay (tradenames) are performed using the Seahorse XFe96 Analyzer (Agilent) with Seahorse XF RPMI Medium (without phenol red) (Agilent). This is an RPMI-based medium added with 10 mM D-glucose (Sigma Aldrich), 1 mM pyruvate (Sigma Aldrich), 2 mM glutamine (Sigma Aldrich) and 1 mM HEPES (Sigma Aldrich), adjusted to pH 7.4, and passed through a 0.2 µm filter (SARSTEDT). On the day of measurement, cells were collected and washed twice with Seahorse XF RPMI Medium (without phenol red). Subsequently, cells were resuspended in Seahorse XF RPMI Medium (without phenol red), seeded in a Seahorse 96-well plate (Agilent, 0.25 Mio/well, at least 8 duplicates) and incubated at 37 °C in a non-CO_2 incubator for 1h. OCR and PER were measured in the Seahorse XFe96 Analyzer. For the Mito Stress Test (**Figure 2-2**), the following compounds were injected sequentially: oligomycin (ATP synthase inhibitor), carbonyl cyanide-p-trifluoromethoxyphenylhydrazone (FCCP, uncoupler of oxidative phosphorylation) and rotenone (Rot, mitochondrial complex I inhibitor) + Antimycin A (AA, mitochondrial complex III inhibitor) (all compounds were from Sigma Aldrich).

Oligomycin was dissolved in DMSO (Sigma Aldrich) at a stock solution of 2 mM, stored in -20 °C, pre-diluted in Seahorse XF RPMI Medium (without phenol red) at a concentration of 20 µg/ml, and finally used at a final concentration of 2 µg/ml.

FCCP was dissolved in DMSO at a stock solution of 15 mM, stored at -20 °C, pre-diluted in Seahorse XF RPMI Medium (without phenol red) at a concentration of 15 µg/ml, and used at a final concentration of 1.5 µg/ml.

Rotenone was dissolved in DMSO at a stock solution of 5 mM, stored at -20 °C, pre-diluted in Seahorse XF RPMI Medium (without phenol red) at a concentration of 5 µg/ml,

and used at a final concentration of 0.5 µg/ml. Antimycin A was dissolved in DMSO at a stock solution of 5 mM, stored at -20 °C, pre-diluted in Seahorse XF RPMI Medium (without phenol red) at a concentration of 5 µg/ml, and used at a final concentration of 0.5 µg/ml.

Parameters were calculated as shown below:

Non-mitochondrial respiration: rotenone and antimycin A exemplify a mitochondrial complex I inhibitor and a complex III inhibitor, respectively. Non-mitochondrial respiration is an OCR that remains after ETC in mitochondria completely inhibited by rotenone and antimycin A, and oxygen consumption takes place from outside of the mitochondria. Non-mitochondrial respiration equates to the average amount of OCRs after rotenone and antimycin A addition.

Basal respiration: Basal respiration is an indicator of basal OXPHOS, and represents the baseline mitochondrial demand of oxygen. Basal respiration comprises the OCR used to produce cellular ATP and mitochondrial proton leak. Basal respiration equals the last OCR before addition of oligomycin minus the non-mitochondrial respiration.

Maximal respiration: Maximal respiration is the maximal capacity with which mitochondria can consume oxygen generated by injection of the uncoupler FCCP. The latter is a protonphore and disrupts the ATP synthesis by transporting protons through the mitochondrial inner membrane. Maximal respiration equals the average amount of OCRs after FCCP addition minus the non-mitochondrial respiration.

ATP production: ATP production is part of the basal respiration used for ATP generation, and ascertained by adding the ATP synthase inhibitor oligomycin. ATP production equals the last OCR before oligomycin addition minus the average amount of OCRs after oligomycin addition).

Proton leak: Proton leak is the proton transport across the mitochondria inner membrane without any ATP generation. Proton leak equals the average amount of OCRs after oligomycin addition minus the non-mitochondrial respiration.

Spare Respirator Capacity (SRC): SRC is the mitochondria reserve capacity indicating a mitochondrial 'response to energy challenge'. Spare Respiratory Capacity equals the maximal respiration minus the basal respiration.

Spare Respiratory Capacity % (SRC%): SRC% equates to the maximal respiration divided by the basal respiration (total values are given in percent).

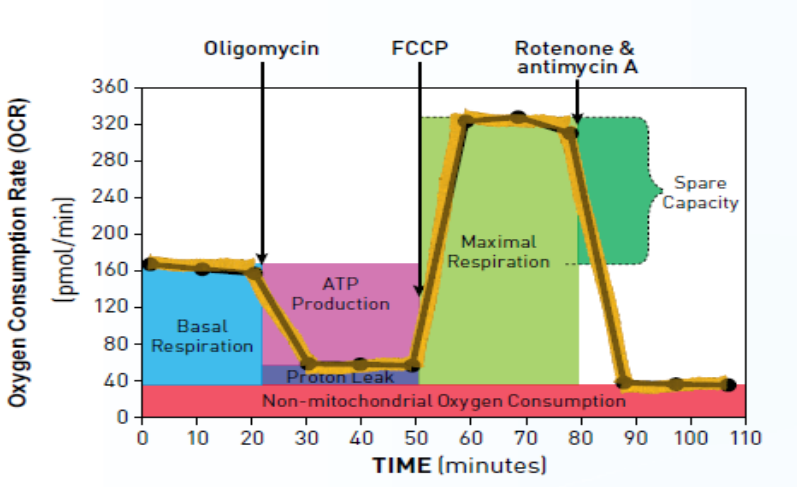

Figure 2-2: Seahorse XF Cell Mito Stress Test kinetic profile and main parameters of mitochondrial respiration (Taken from agilent.com).

For the Glycolytic Rate Assay **(Figure 2-3**), the compounds' final concentrations were: 0.5 µM rotenone + 0.5 µM antimycin A and 50 mM 2-deoxy-glucose (2-DG, glycolytic inhibitor) (all compounds were from Sigma Aldrich) and parameters were calculated as shown below:

Basal Proton efflux rate (PER): basal PER indicates the protons secreted by cells over time before the compound was added. Basal PER equals the last proton efflux rate before rotenone and antimycin A addition.

Mitochondrial acidification (mito acidification**) or Mitochondrial PER (**Mito PER**):** This is the CO_2 initiated in the TCA cycle in mitochondria which contributes to extracellular acidification, and results in an additional proton efflux rate beyond that generated by glycolysis. Mito acidification/Mito PER can be calculated by measuring OCR simultaneously. Basal mito acidification/Mito PER equals the basal respiration multiplied by the CO_2 contribution factor (CCF).

Glycolytic efflux rate (glycoPER): the glycolytic efflux rate is the number of protons extruded into the Seahorse XF RPMI Medium (without phenol red) from glycolysis. Basal glycoPER equals basal proton efflux rate (PER) minus Mito PER.

Compensatory glycolysis: Compensatory glycolysis is the cell compensatory capacity utilizing glycolysis while OxPhos is totally shut down by rotenone and antimycin A. Compensatory glycolysis equals the average of PER after rotenone and antimycin A addition.

Post-2-DG acidification: Post-2-DG acidification is a residual extracellular acidification after inhibition of glycolysis and mitochondrial OxPhos. It represents other sources of proton generation but not a complete inhibition of any remaining glycolysis by 2-DG. Post-2-DG acidification equals the last PER measurement after addition 2-DG.

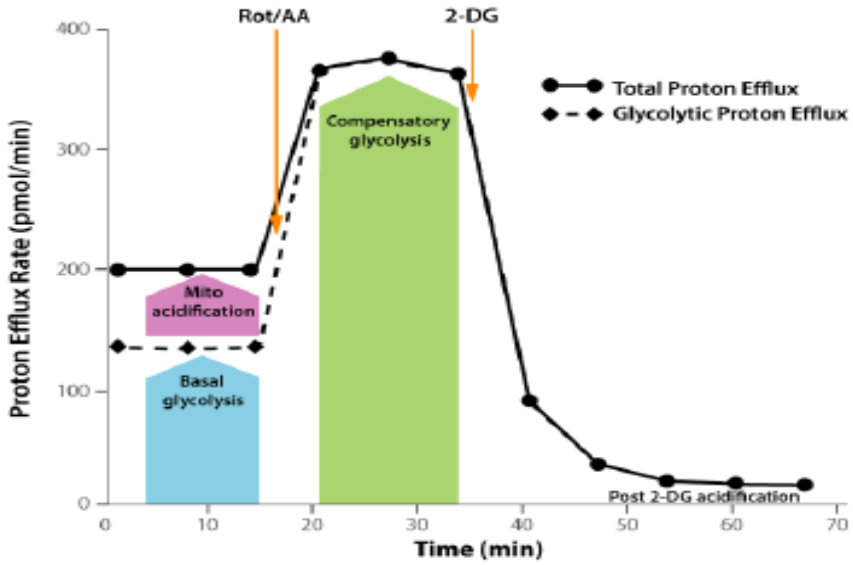

Figure 2-3: Seahorse XF Glycolytic Rate kinetic profile and mainly glycolytic parameters (Taken from agilent.com).

Cellular OCR and PER were measured four times to obtain a basal line, and after subsequent injection. Data were acquired and analyzed by use of the Wave software (Agilent).

2.2.6. Multiplex ELISA

Cells were stimulated by incorporating T Cell TransAct™ (Miltenyi Biotec) supplemented with IL-2 in RPMI 1640 medium with 5% human AB Serum, and 1% penicillin/streptomycin. The cell number was adjusted to a final concentration of $2x10^6$

/ml, seeded in 200-µl lots in every well of a 96-well flat bottom plate. Supernatants of cultured cells at the beginning and after 24 h of T Cell TransAct™ stimulation were collected and kept at -20 °C until measurement. The supernatants were measured for IL-1ra, IL-2, IL-4, IL-5, IL-6, IL-8, IL-9, IL-10, IL-13, IL-17, GM-CSF, IFN-γ, IP-10, MCAF, MIP-1a, MIP-1b, RANTES, TNF-α, and VEGF in a Bio-Plex suspension system (Bio-Rad) according to the manufacturer's instructions. Suspensions were diluted 1-to-1 using relevant buffers.

2.3. Statistics

Statistics were analyzed with GraphPad® Prism software (GraphPad Software, La Jolla, USA). Data were analyzed for normal distribution with the Shapiro–Wilk test and Kolmogorov-Smirnov-Test. Mann-Whitney U test and unpaired t test (with Welch's correction in data without equal variances) were used for independent data; paired t test or Wilcoxon signed-rank test were used for dependent data. P values of <0.05 were assumed to be statistically significant. The following symbols were used: * for P<0.05, ** for P<0.01, and *** for P<0.001.

3. Results

3.1. Highly purified human naive CD4⁺ T cells and memory CD4⁺ T cells were obtained

After depletion of naive $CD4^+$ by use of the Naïve cell Isolation Kit II and/or Memory $CD4^+$ T Cell Isolation Kit, followed by a positive selection by $CD4^+$ microbeads, the purity of naive $CD4^+$ T cells and memory $CD4^+$ T cells was checked by flow cytometry. The representative example provided below showed that 92.4% of the naive $CD4^+$ T cells, and 93.8 % of the memory $CD4^+$ T cells were viable. After excluding debris and dead cells, 98.8% of the naive $CD4^+$ T cells were CD3 positive and CD4 positive, and 99.4% of the memory $CD4^+$ T cells were CD3 positive and CD4 positive. Out of the CD3 and

CD4-positive population, naive CD4⁺ T cells showed a 95.6%-CD45RO negative and CD45RA-positive population, while memory cells had a 98.2%-CD45RO positive and CD45RA-negative population (**Figure 3-1**).

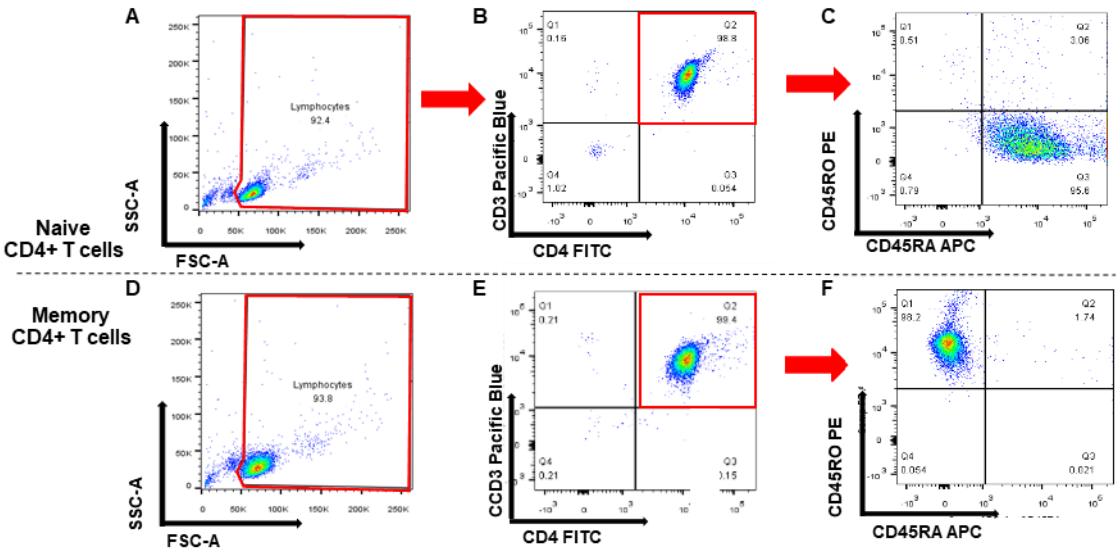

Figure 3-1: Flow cytometric control of isolated human naive and memory CD4⁺ T cells. Representative example of flow cytometric gating strategy on naive and memory CD4⁺ T cells. (A) Gate live cells from whole population of naive CD4⁺ T cells; (B) Gate CD3-positive and CD4-positive population of live cells; (C) Gate CD45RO-negative and CD45RA-positive population of CD3-positive and CD4-positive fractions. (D) Gate live cells of whole populations of memory CD4⁺ T cells; (E) Gate CD3-positive and CD4-positive population of live cells; (F) Gate CD45RO-negative and CD45RA-positive population of CD3-positive and CD4-positive fraction (representative for one donor).

3.2. *Ex vivo* cellular metabolism as determined by the Seahorse Analyzer

3.2.1. Metabolism in naive and memory CD4⁺ T cells

To clarify phenotypes of mitochondrial function and glycolysis in naive and memory CD4⁺ T cells, and to compare the differences between these two groups, we isolated naive and memory CD4⁺ T cells from 18 filters (**Table 3-1**). Using the isolated cell fractions, we performed Mito Stress Test and Glycolytic Rate assays using the Seahorse XFe 96 Analyzer.

Table 3-1: Data of filters used for Seahorse XFe 96 Analyzer measurements. Due to data protection, only the following information is shown. Donor data were retrieved from the records stored at the blood donation department of Charité – Universitätsmedizin Berlin.

Filter number	Gender	Age (years)	Group
18001991	Female	32	Young
18002066	Male	54	Aged
18002067	Male	25	Young
18002230	Male	63	Aged
18002233	Female	26	Young
18002505	Male	65	Aged
18002511	Male	23	Young
18002599	Male	67	Aged
18002602	Female	26	Young
18002783	Male	52	Aged
18002778	Male	22	Young
18002857	Male	20	Young
18003207	Female	53	Aged
18003204	Male	27	Young
18003315	Female	57	Aged
18003320	Male	24	Young
18003430	Female	55	Aged
18003436	Male	54	Aged

3.2.1.1. Memory $CD4^+$ T cells have a substantially higher basal respiration and reserve capacity to use oxygen than naive cells do

We measured the OCR of isolated $CD4^+$ naive and memory T cells, both under basal conditions and after injection of oligomycin, FCCP, and rotenone and antimycin A (**Figure 3-2 A**). As shown in **Figure 3-2 B**, basal OCR of memory $CD4^+$ T cells was 33.52 ± 6.57 pmol/min, and thus significantly higher than that of $CD4^+$ naive T cells which was 25.96 ± 6.28 pmol/min (P=0.0005). After addition of FCCP, memory $CD4^+$ T cells showed a significantly higher increase of maximal respiration (139.70 ± 31.46 pmol/min) as compared to $CD4^+$ naive T cells (90.15 ± 22.22 pmol/min, P<0.0001). SRC or respiratory capacity indicates the mitochondrial reserve capacity, which was significantly higher in memory $CD4^+$ T cells (106.2 ± 26.34 pmol/min) than it was in $CD4^+$ naive T cells (64.07 ± 17.95 pmol/min, P<0.0001). Moreover, SRC% was also significantly higher in memory $CD4^+$ T cells when compared to $CD4^+$ naive T cells (424.4 ± 54.73% and 353.5 ± 59.97%, respectively, P=0.001) (**Figure 3-2 C**). Memory $CD4^+$ T cells also demonstrated higher values for (i) non-mito OCR (19.84 ± 3.789 pmol/min), (ii) ATP production (25.16 ± 5.422 pmol/min), and (iii) proton leak (8.357 ± 2.415 pmol/min) than do naive $CD4^+$ T cells which yielded the values 13.96 ± 2.569 pmol/min, (P<0.0001), 20.04 ± 4.719 pmol/min (P=0.0012) and 6.040 ± 2.536 pmol/min (P=0.0012), respectively. However, these two groups did show the same coupling efficiency (**Figure 3-2 D**). These data demonstrate that memory $CD4^+$ T cells not only have a higher basal respiration but also a higher reserve mitochondrial capacity to use oxygen, when compared to naive $CD4^+$ T cells.

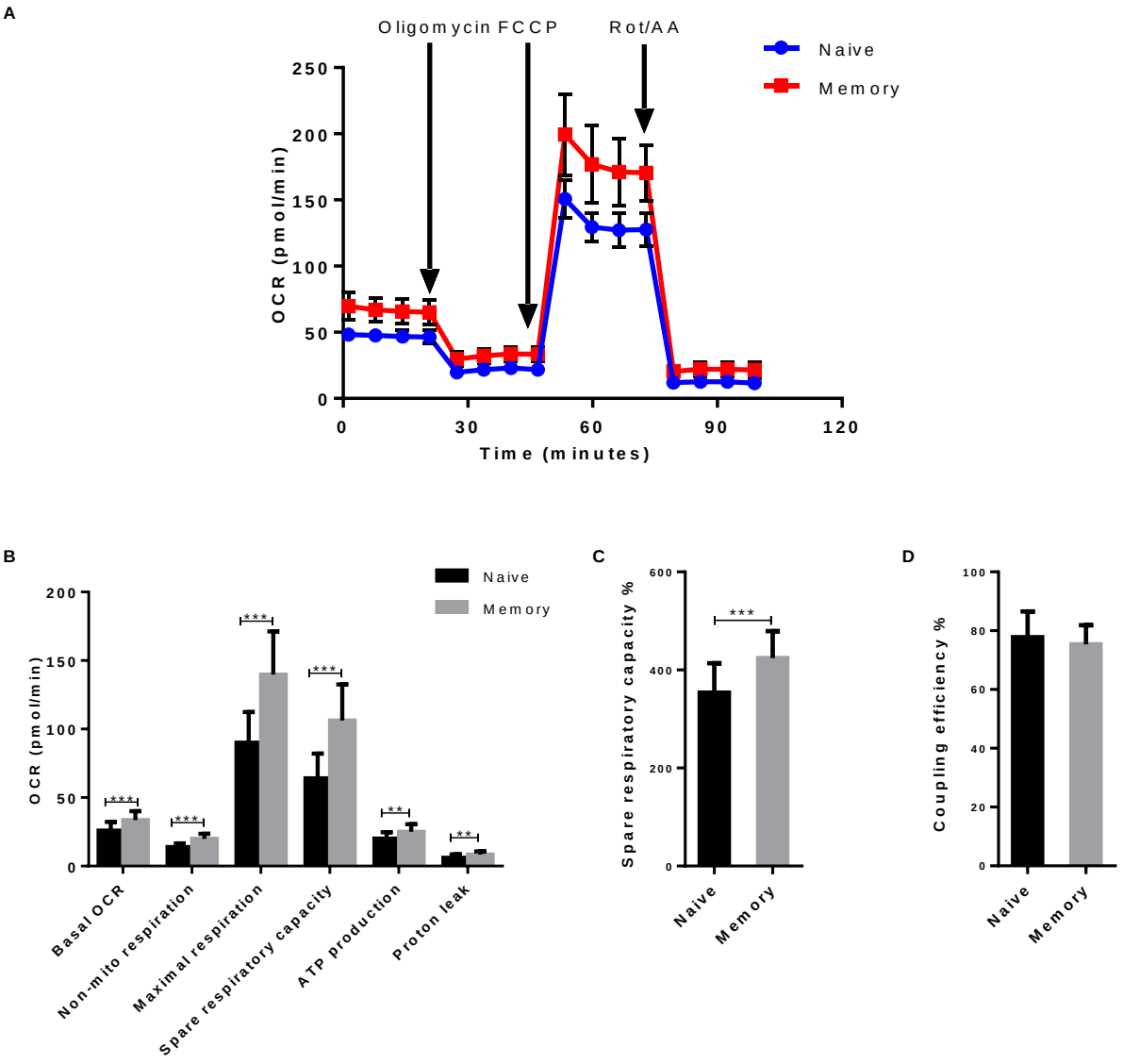

Figure 3-2: Differences in mitochondrial function between naive and memory CD4⁺ T cells. Naive and memory CD4⁺ T cells were measured in regard to OCR under basal conditions and after injections of oligomycin, FCCP, and Rot/AA. (A) Representative example of the Seahorse XF Cell Mito Stress Test kinetic profile of naive and memory CD4⁺ T cells. (B) Comparison of basal OCR, non-mito respiration, maximal respiration, spare respiratory capacity, ATP production, proton leak between naive and memory CD4⁺ T cells. (C) Comparison of spare respiratory capacity% between naive and memory CD4⁺ T cells. (D) Comparison of coupling efficiency between naive and memory CD4⁺ T cells. Data are shown as mean ± SD. A paired t test or Wilcoxon signed-rank test was performed after the normality test. N=18 individual donors in each group. **P<0.01; ***P<0.001.

3.2.1.2. Memory $CD4^+$ T cells have a higher basal glycolysis and compensatory glycolysis than naive cells do

As a measure of glycolytic flux, we analyzed the PER of isolated naive and memory $CD4^+$ T cells, both under basal conditions and after injections of Rot/AA, and 2-DG (**Figure 3-3 A**). Using the glycolytic rate assay, memory $CD4^+$ T cells demonstrated significantly higher basal glycolysis (glycoPER) (91.46 ± 33.14 pmol/min) than naive $CD4^+$ T cells did (61.43 ± 24.21 pmol/min, P=0.0004) (**Figure 3-3 B**). According to basal glycolysis, memory $CD4^+$ T cells also had a significantly higher compensatory glycolysis (145.0 ± 39.87 pmol/min) when compared to naive $CD4^+$ T cells (104.1 ± 24.48 pmol/min, P=0.0009). In addition, basal PER and the post 2-DG acidification rate of memory $CD4^+$ T cells also demonstrated a statistically significant difference when compared to naive $CD4^+$ T cells (115.8 ± 34.39 pmol/min and 79.54 ± 23.21 pmol/min; 39.39 ± 7.61 pmol/min and 27.08 ± 7.02 pmol/min, respectively) (P=0.0001 and P<0.0001, respectively). Conversely, naive and memory $CD4^+$ T cells did not differ significantly in their ratios of basal mitoOCR/glycoPER (**Figure 3-3 C**).

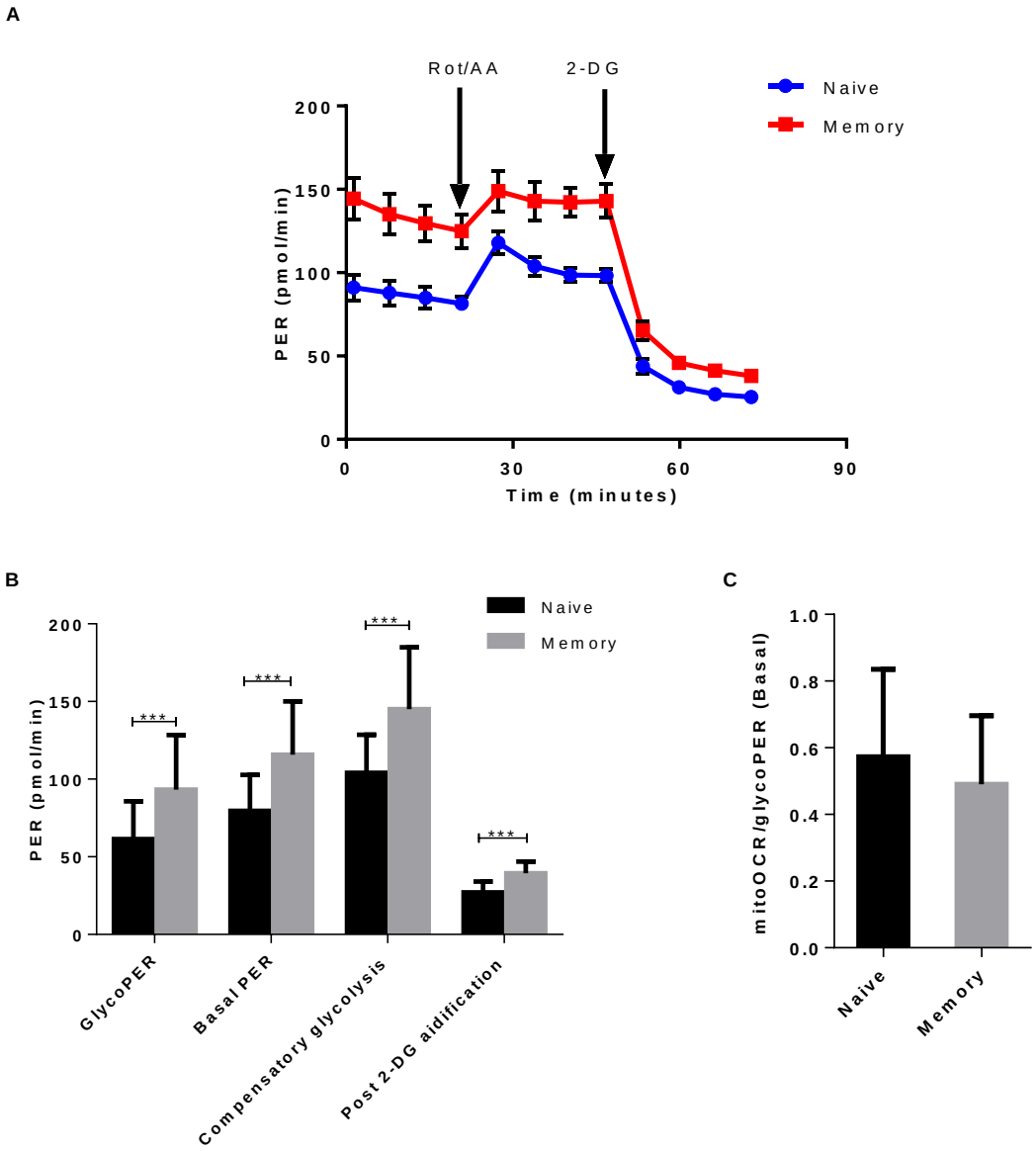

Figure 3-3: Differences of glycolytic function between naive and memory CD4⁺ T cells. Naive and memory CD4⁺ T cells were measured in respect to PER under basal conditions and after injections of Rot/AA and 2-DG. (A) Representative example of Seahorse XF Glycolytic Rate kinetic profile of naive and memory CD4⁺ T cells. (B) Comparison of basal glycolysis, basal PER, compensatory glycolysis and post 2-DG acidification rate between naive and memory CD4⁺ T cells. (C) Comparison of basal mitoOCR/glycoPER ratio between naive and memory CD4⁺ T cells. Data are shown as mean ± SD. A paired t test was performed after the normality test. N=18 individual donors in each group. ***P<0.001.

Taken together, memory CD4⁺ T cells demonstrated higher basal respiration, SRC, glycolysis, compensatory glycolysis in comparison with naive CD4⁺ T cells, but a similar mitoOCR/glycoPER ratio, indicating that there is a higher metabolic flux in memory CD4⁺

T cells than in naive $CD4^+$ T cells.

3.2.2. Naive $CD4^+$ T cells from young donors and aged donors demonstrate the same metabolic phenotype.

In order to further demonstrate the metabolic phenotype of naive $CD4^+$ T cells in young donors and aged donors, we analyzed 9 young and 9 aged gender-matched donors (**Table 3-2**).

Table 3-2: Characters of young and aged donors in Seahorse XFe 96 Analyzer measurements

	Age (years)	Age (years, mean ± SD)	Male: Female
Young (n=9)	20-32	25.0 ± 3.4	6:3
Aged (n=9)	52-67	57.8 ± 5.7	6:3

There was a trend that naive $CD4^+$ T cells from aged donors displayed higher values for basal OCR, maximal respiration, SRC, SRC%, ATP production, and proton leak when compared to naive $CD4^+$ T cells from young donors (**Figure 3-4 A, B**), although here, no statistical significance was observed. They also show a similar coupling efficiency (**Figure 3-4 C**).

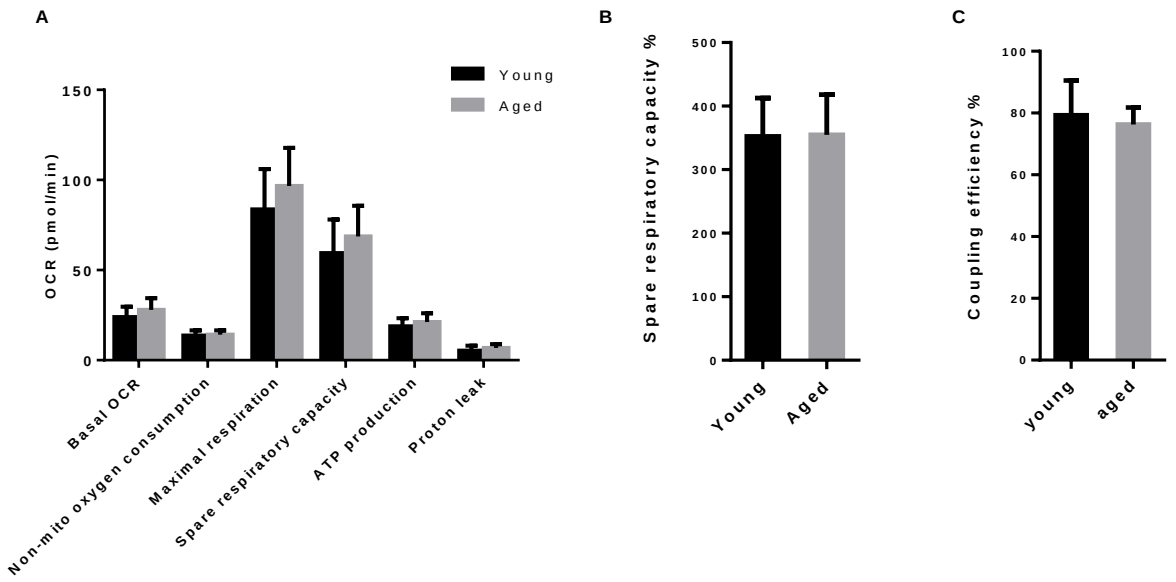

Figure 3-4: Naive CD4⁺ T cells from young donors and aged donors have the same mitochondrial metabolic phenotype. Naive CD4⁺ T cells from young and aged donors were measured to investigate OCR under basal conditions and after injections of oligomycin, FCCP and Rot/AA. (A) Comparison of basal OCR, non-mito respiration, maximal respiration, spare respiratory capacity, ATP production, proton leak in naive CD4⁺ T cells from young donors and aged donors. (B) Comparison of spare respiratory capacity% in naive CD4⁺ T cells from young donors and aged donors. (C) Comparison of coupling efficiency in naive CD4⁺ T cells from young donors and aged donors. Data are shown as mean ± SD. An unpaired t test was performed after the normality test. N=9 individual donors in each group.

For the Glycolytic Rate Assay, naive CD4⁺ T cells from young and aged groups showed no differences in basal glycoPER, basal PER, compensatory glycolysis, post 2-DG acidification rate or ratio of basal mitoOCR/glycoPER (**Figure 3-5 A, B**). Therefore, we conclude that naive CD4⁺ T cells from young and aged donors have a similar metabolic phenotype.

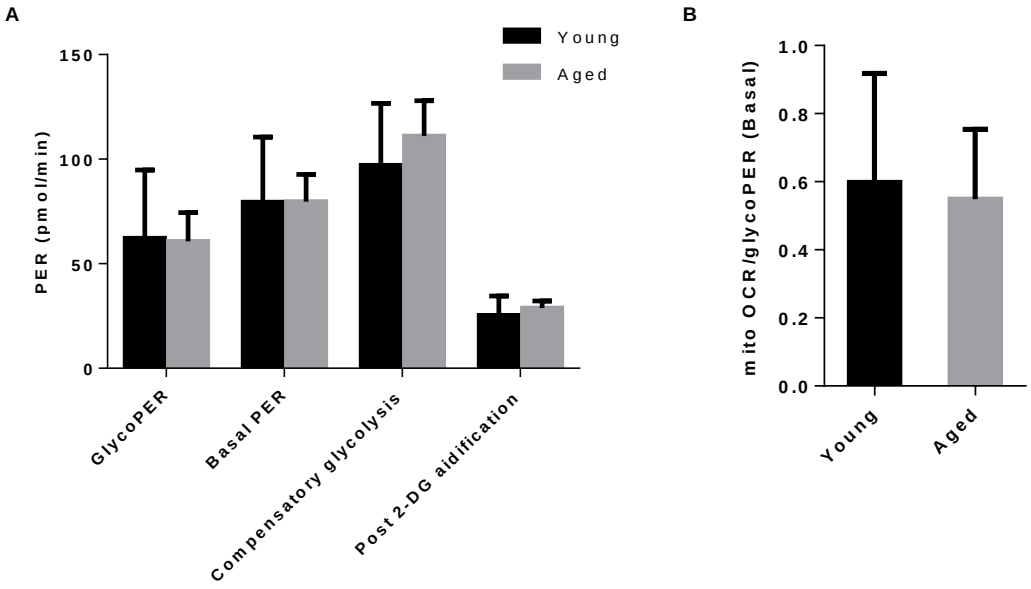

Figure 3-5: Naive CD4⁺ T cells from young donors and aged donors have the same glycolytic metabolic phenotype. Naive CD4⁺ T cells were measured for PER under basal conditions and after injections of Rot/AA, and 2-DG. (A) Comparison of basal glycolysis, basal PER, compensatory glycolysis and post 2-DG acidification rate in naive CD4⁺ T cells from young donors and aged donors. (B) Comparison of basal mitoOCR/glycoPER ratio in naive CD4⁺ T cells from young donors and aged donors. Data are shown as mean ± SD. An unpaired t test was performed after the normality test. N=9 individual donors in each group.

3.2.3. Metabolism of memory CD4⁺ T cells in young donors and aged donors

Focusing on memory CD4⁺ T cells, we continued to investigate whether young donors and aged donors differ in their metabolic phenotype. After analyzing the mitochondrial metabolic parameters in memory CD4⁺ T cells, we observed no statistical difference in basal OCR, non-mito OCR, maximal respiration, SRC, ATP production, proton leak, percentage of SRC, or coupling efficiency between the two groups (**Figure 3-6**).

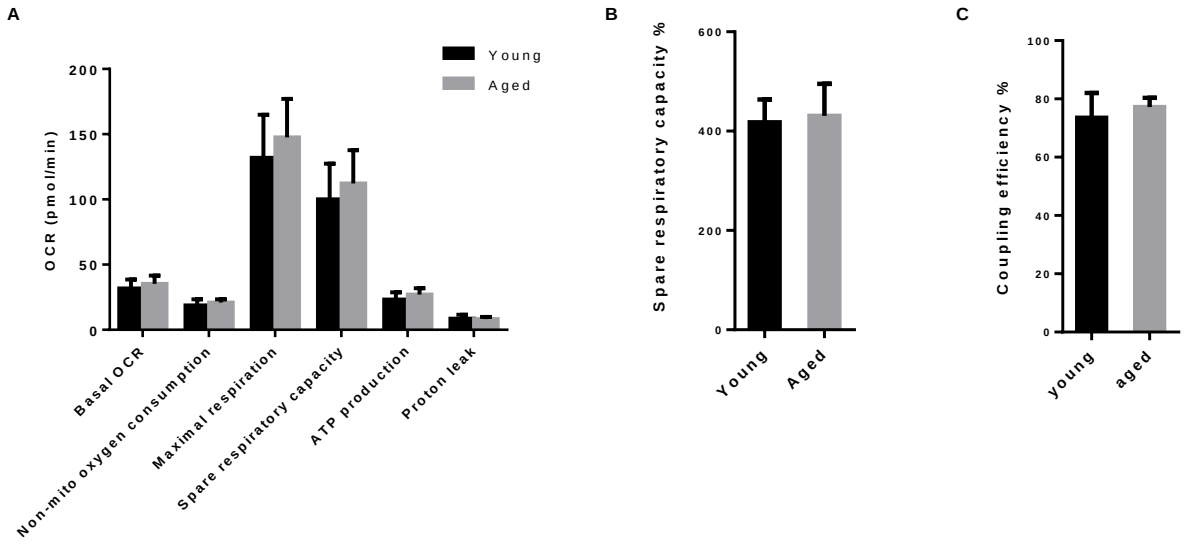

Figure 3-6: Mitochondrial profiles of memory CD4⁺ T cells in young donors and aged donors. Memory CD4⁺ T cells from young and aged donors were measured for OCR under basal conditions and after injections of oligomycin, FCCP, and Rot/AA. (A) Comparison of basal OCR, non-mito respiration, maximal respiration, spare respiratory capacity, ATP production, proton leak in memory CD4⁺ T cells from young donors and aged donors. (B) Comparison of spare respiratory capacity% in memory CD4⁺ T cells from young donors and aged donors. (C) Comparison of coupling efficiency in memory CD4⁺ T cells from young donors and aged donors. Data are shown as mean ± SD. Unpaired t test and Mann-Whitney test were performed after the normality test. N=9 individual donors in each group.

It is of interest that basal glycolysis (glycoPER) of memory CD4⁺ T cells from aged donors (73.5 ± 19.17 pmol/min) was lower than it was in young donors (109.4 ± 35.22 pmol/min, P=0.0162) (**Figure 3-7 A**). After blocking mitochondrial respiration, memory CD4⁺ T cells from aged donors demonstrated a significantly lower compensatory glycolysis (126.1 ± 21.47 pmol/min) than memory CD4⁺ T cells from young donors did (163.9 ± 45.98 pmol/min, P=0.0468). These two groups also showed statistically significant differences in basal PER (young group: 133.1 ± 38.59 pmol/min, aged group: 98.36 ± 18.52 pmol/min). Accordingly, memory CD4⁺ T cells of aged donors demonstrated a significantly higher ratio of basal mitoOCR/glycoPER (0.38 ± 0.15) than those from young donors (0.59 ± 0.21 pmol/min, P=0.0227) (**Figure 3-7 B**). These findings indicate that memory CD4⁺ T cells from aged donors have lower basal glycolysis and compensatory glycolysis than those from young donors, and that this leads to a decline in the ability of using glycolysis. In order to exclude any hormonal effect of females, we analyzed all of the above-

mentioned metabolic data from males only. The findings obtained confirmed the previous results from the gender-matched groups (data not shown).

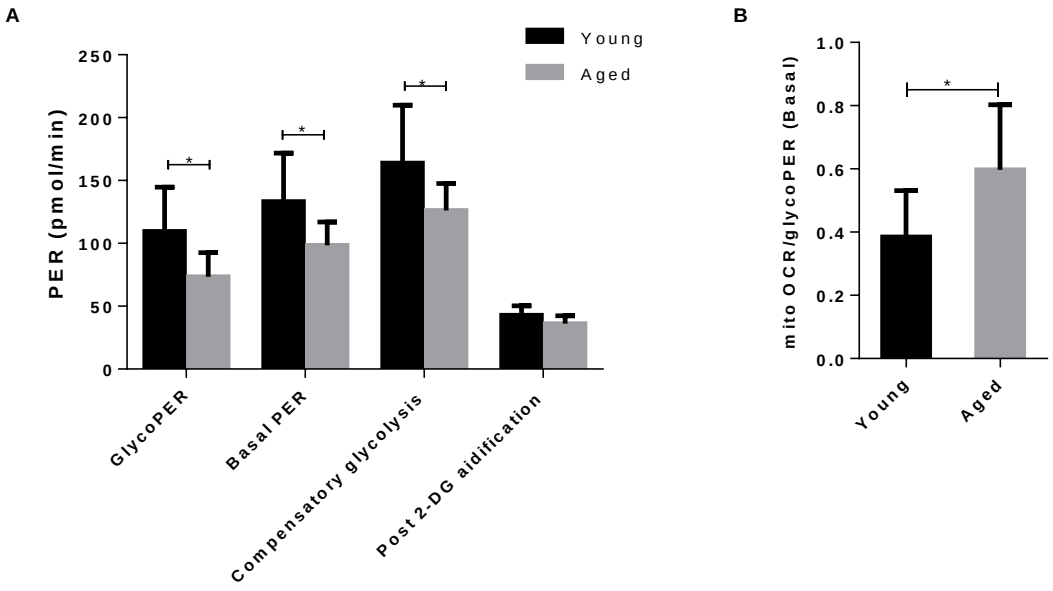

Figure 3-7: Glycolytic profiles of memory CD4⁺ T cells in young donors and aged donors. Memory CD4⁺ T cells were measured in respect to PER under basal conditions and after injections of Rot/AA, and 2-DG. (A) Comparison of basal glycolysis, basal PER, compensatory glycolysis and post 2-DG acidification rate between naive CD4⁺ T cells from young donors and aged donors. (B) Comparison of basal mitoOCR/glycoPER ratio between memory CD4⁺ T cells from young donors and aged donors. Data are shown as mean ± SD. An unpaired t test was performed after the normality test. N=9 individual donors in each group. *P<0.05.

3.2.4. Glycolysis of naive and memory CD4⁺ T cells from young donors

Finally, we compared glycolysis between naive and memory CD4⁺ T cells in young donors. In line with our findings, we observed in all donors analyzed (young and aged donors), that naive and memory CD4⁺ T cells demonstrated significant differences in basal glycolysis, basal PER, compensatory glycolysis and post 2-DG acidification rates (109.4 ± 35.22 versus 62.16 ± 32.65 pmol/min, 133.1 ± 38.59 versus 79.38 ± 31.23 pmol/min, 163.9 ± 45.98 versus 97.09 ± 29.64 pmol/min, and 42.71 ± 7.638 versus 25.33 ± 9.282 pmol/min, respectively; P=0.0011, 0.0011, 0.0014, and 0.0002, respectively) (**Figure 3-8**

A). Memory CD4$^+$ T cells of young donors showed a lower ratio of basal mitoOCR/glycoPER (0.38 ± 0.15) than that of aged donors (0.60 ± 0.32, P=0.0330) (**Figure 3-8 B**)

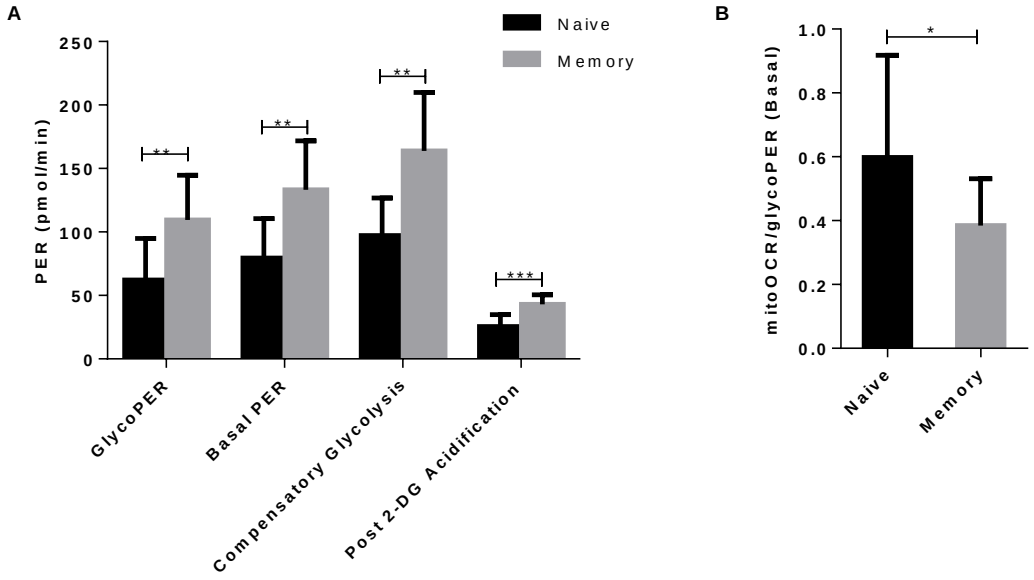

Figure 3-8: Glycolytic profiles of naive and memory CD4$^+$ T cells in young donors. Naive and memory CD4$^+$ T cells were measured for PER under basal conditions and after injections of Rot/AA, and 2-DG. (A) Comparison of basal glycolysis, basal PER, compensatory glycolysis and post 2-DG acidification rates between naive and memory CD4$^+$ T cells. (B) Comparison of basal mitoOCR/glycoPER ratio between naive and memory CD4$^+$ T cells. Data are shown as mean ± SD. A paired t test was performed after the normality test. N=9 individual donors in each group. ***P<0.05, ***P<0.01, ***P<0.001.

3.2.5. Glycolysis of naive and memory CD4$^+$ T cells from aged donors

Among aged donors, statistical differences in basal glycolysis, compensatory glycolysis and the ratio basal mitoOCR/glycoPER between memory CD4$^+$ T cells and naive CD4$^+$ T cells practically disappear (**Figure 3-9 A**). Nonetheless, basal PER and post 2-DG acidification rates were higher in memory CD4$^+$ T cells (98.36 ± 18.52 and 36.07 ± 6.30 pmol/min, respectively) than they were in naive CD4$^+$ T cells (79.70 ± 13.01 and 28.83 ± 3.42 pmol/min, respectively). P-values for the memory and naive cell types were 0.0113

and 0.0082, respectively. (**Figure 3-9 B**).

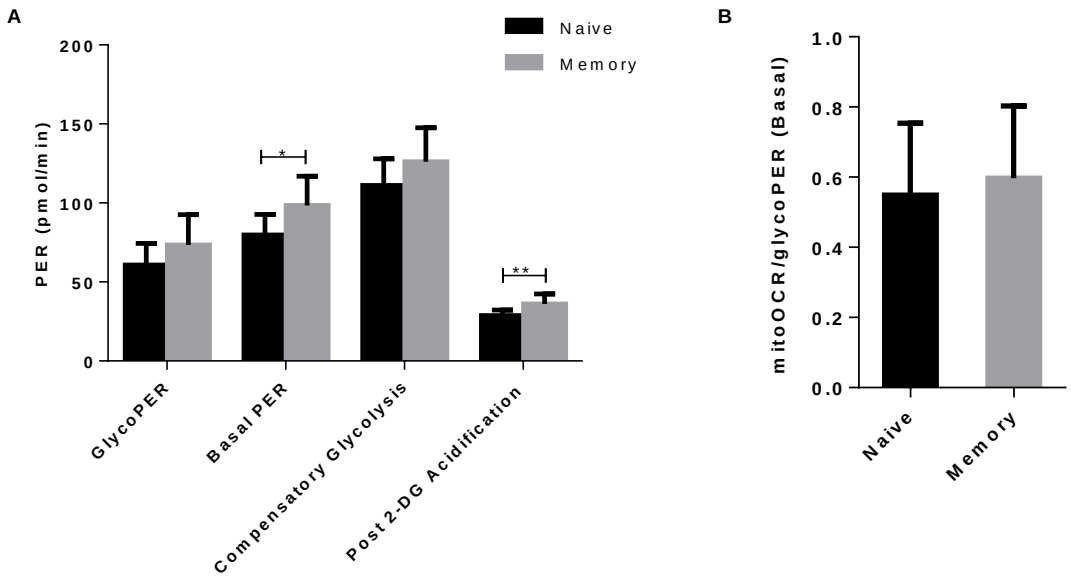

Figure 3-9: Glycolytic profiles of naive and memory CD4⁺ T cells in aged donors. Naive and memory CD4⁺ T cells were measured for PER under basal conditions and after injections of Rot/AA, and 2-DG. (A) Comparison of basal glycolysis, basal PER, compensatory glycolysis and post 2-DG acidification rates between naive and memory CD4⁺ T cells. (B) Comparison of basal mitoOCR/glycoPER ratios between naive and memory CD4⁺ T cells. Data are shown as mean ± SD. A paired t test was performed after the normality test. N=9 individual donors in each group. *P<0.05, ***P<0.01.

To summarize at this point, we conclude that the differences in basal glycolysis and compensatory glycolysis observed in the young population between naive and memory CD4⁺ T cells contribute to the differences seen in the whole population.

3.2.6. Metabolism of naive or memory CD4⁺ T cells in female donors and male donors

Focusing on gender-dependent metabolic differences in T cells, we analyzed the metabolic phenotypes of naive and memory CD4⁺ T cells from female donors and then compared these with those from male donors. For this, we used blood from 6 female donors and 6 age-matched male donors (**Table 3-3**, **Table 3-4**). In naive CD4⁺ T cells, male donors demonstrated a higher basal OCR (29.22 ± 6.98 pmol/min), maximal respiration (107.8 ± 20.04 pmol/min), spare respiratory capacity (78.55 ± 14.56 pmol/min),

ATP production (23.00 ± 5.01 pmol/min), and mitoOCR/glyco PER(Basal) (0.74 ± 0.27 pmol/min) when compared to female donors (21.50 ± 3.95 pmol/min, 80.91 ± 13.52 pmol/min, 59.41 ± 11.54 pmol/min, 16.82 ± 2.67, and 0.44 ±0.26 pmol/min. (Corresponding P-values were 0.0402, 0.0411, 0.0152, 0.0236, and 0.0260 respectively). In respect to memory $CD4^+$ T cells, female donors and male donors did not demonstrate any apparent statistical differences in all parameters of mitochondrial and glycolytic profile.

Table 3-3: Data of filters used for metabolic comparison between female donors and male donors. Due to data protection, only following information is shown. Donor data were retrieved from records taken from the blood donation department of Charité – Universitätsmedizin Berlin.

Filter number	Gender	Age (years)
18001991	Female	32
18002233	Female	26
18002602	Female	26
18003207	Female	53
18003315	Female	57
18003430	Female	55
18002066	Male	54
18002067	Male	25
18002230	Male	63
18002783	Male	52
18003204	Male	27
18003320	Male	24

Table 3-4: Characters of female and male donors in Seahorse XFe 96 Analyzer measurements

	Age (years)	Age (years, mean±SD)
Female (n=6)	26-57	41.5±6.2
Male (n=6)	24-63	40.8±7.1

3.3. Proliferation and cytokine production/secretion in memory CD4$^+$ T cells

Metabolism does affect immune cell function. Since our results indicate that memory CD4$^+$ T cells from young donors differ in basal glycolysis, basal PER and compensatory glycolysis, we asked ourselves whether or not metabolism has any influence on specific functions of memory CD4$^+$ T cells. In this regard, we investigated activation-induced cell proliferation and cytokine production of memory CD4$^+$ T cells. Since the male population had the same metabolic phenotype in memory CD4$^+$ T cells from young and aged donors as the whole population did, we chose male donors in order to exclude any female hormonal effects in the following experiments (**Table 3-5**, **Table 3-6**).

Table 3-5: Data of filters used for functional experiments. Due to data protection, only the following information is shown. Donor data were retrieved from documents taken from the blood donation department of Charité – Universitätsmedizin Berlin.

Filter number	Gender	Age (years)	Group
18007135	Male	29	Young
18007127	Male	67	Aged
18007386	Male	22	Young
18007384	Male	64	Aged
18007938	Male	23	Young
18007933	Male	66	Aged
18008045	Male	29	Young
18008034	Male	63	Aged
18008993	Male	25	Young
18008995	Male	68	Aged
18009113	Male	31	Young
18009114	Male	62	Aged

Table 3-6：Characters of young and aged donors in functional experiments.

	Age (years)	Age (years，mean ± SD)	Male: Female
Young (n=6)	22-31	26.5 ± 3.7	6:0
Aged (n=6)	62-68	65.0 ± 2.4	6:0

3.3.1. Proliferation of memory $CD4^+$ T cells after specific stimulation with anti-human CD3 and CD28 antibodies

For cell proliferation, CD3/28-stimulated memory $CD4^+$ T cell proliferation was determined by flow cytometry, 3 and 4 days after using CSFE and Ki-67 techniques. After CSFE staining, we observed a trend towards a higher proliferation of memory $CD4^+$ T cells from aged persons in comparison to cells from young subjects, but we observed no significant differences in cell division index, proliferation index, and percentage of divided cells as calculated by FlowJo (TreeStar) (**Figure 3-10**). In a manner similar to the results on the CSFE experiments, Ki-67 expression did not differ significantly in both groups (**Figure 3-11**).

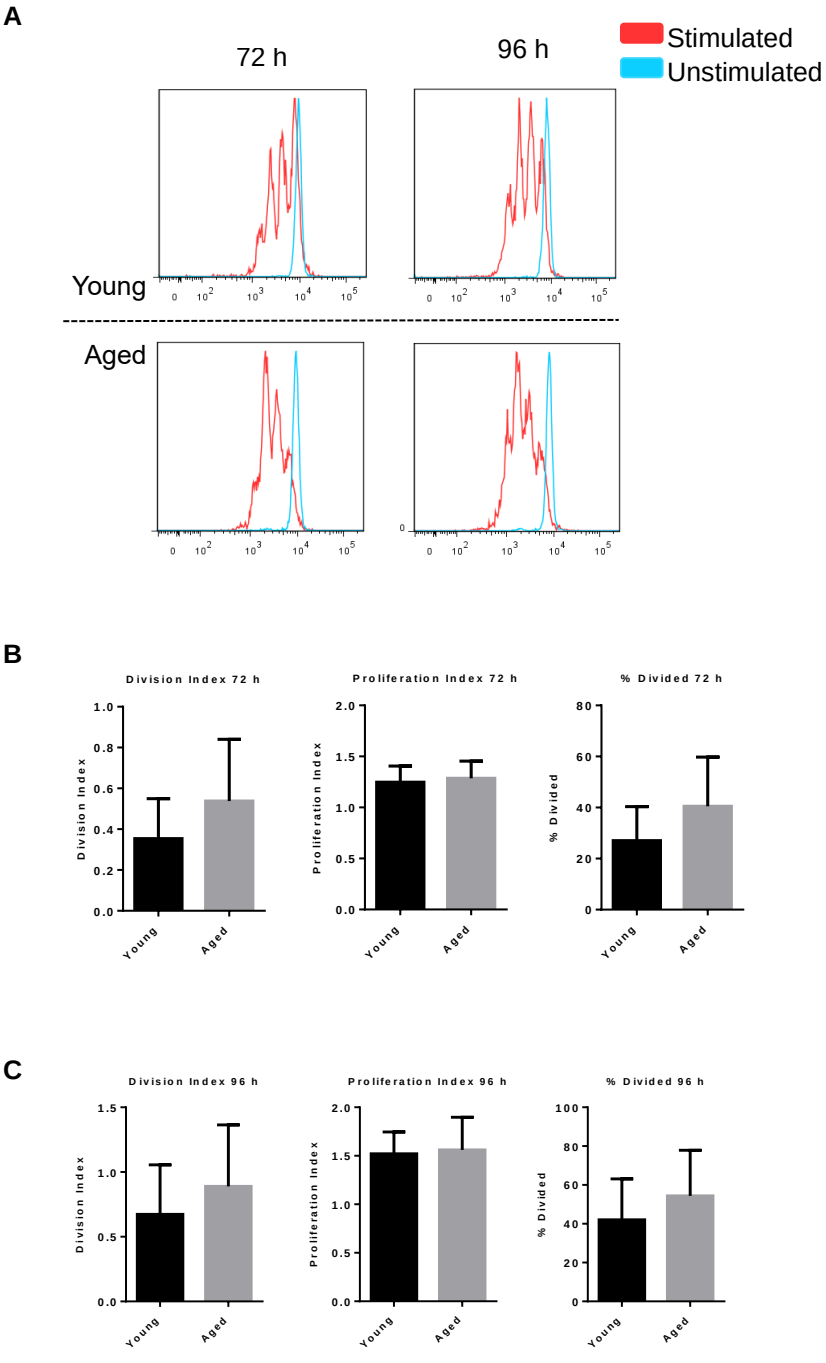

Figure 3-10: Memory CD4⁺ T cell proliferation as determined by CSFE after 72 h or 96 h of TCR stimulation. (A) Representative example of flow cytometric CSFE on memory CD4⁺ T cells from young and aged donors after 72 h and 96 h of TCR stimulation. Comparison of division index, proliferation index, and percentage divided cells (B) between memory CD4⁺ T cells from young donors and aged donors after 72 h of TCR stimulation (n=5 individual donors in each group). Comparison of division index, proliferation index, percentage divided cells (C) between memory CD4⁺ T cells from young donors and aged donors after 96 h of TCR stimulation (n=6 individual donors in each group). Data are shown as mean ± SD. An unpaired t test was performed after the normality test

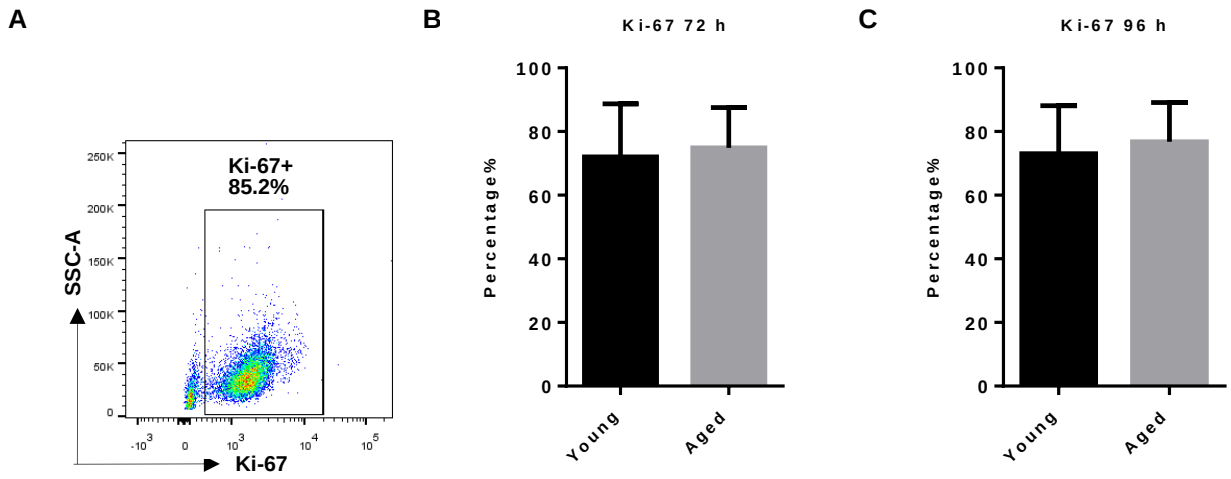

Figure 3-11: Proliferation of memory CD4⁺ T cell as determined by Ki-67 after 72 h or 96 h of TCR stimulation. (A) Representative example of Ki-67 positive memory CD4⁺ T cells acquired by flow cytometry. Comparison of Ki-67 positive cells in memory CD4⁺ T cells from young donors and aged donors after 72 h (B) (n=6 individual donors in each group) and 96 h (C) of TCR stimulation (n=5 individual donors in each group). Data are shown as mean ± SD. An unpaired t test was performed after the normality test.

3.3.2. Cytokine production/secretion in memory CD4⁺ T cells

Intracellular cytokine expression of memory CD4⁺ T cells after stimulation with PMA and ionomycin: An important function of memory CD4⁺ T cells is the production/secretion of cytokines. In order to investigate the effect of glycolysis on the cytokine synthesis of memory CD4⁺ T cells, we checked intracellular cytokine expression after PMA/ionomycin stimulation, and quantified cytokine secretion in supernatants before (0 h) and 24 h after TCR stimulation.

3.3.2.1. Intracellular cytokine expression of memory CD4⁺ T cells after stimulation with PMA and ionomycin

We stimulated memory CD4⁺ T cells using PMA/ionomycin for 5 hours, and determined the expression of IL-2, IL-4, IL-10, IL-17, IFN-γ, and TNF-α using flow cytometry. Data were analyzed for geometric mean fluorescence intensity (gMFI). We found no statistical differences in memory CD4⁺ T cells between young and aged donors (**Figure 3-12**).

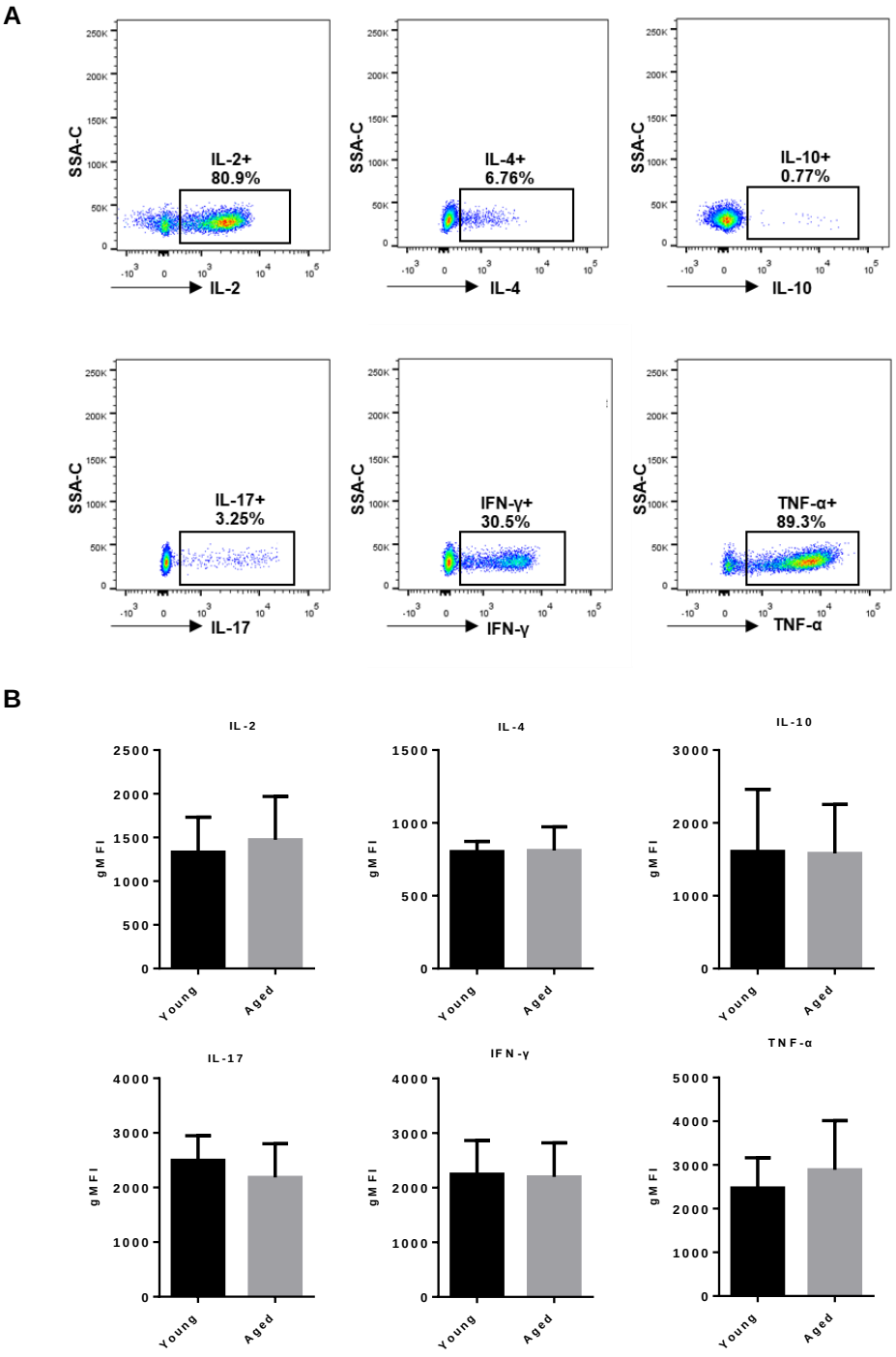

Figure 3-12: Intracellular cytokines expression of memory CD4⁺ T cells. Cells were activated with PMA/ionomycin for 5 h, and during the last 3 hours, BFA was added. (A) Representative example of cytokine expression memory CD4⁺ T cells from young and aged donors acquired by flow cytometry after stimulation. (B) gMFIs of IL-2, IL-4, IL-10, IL-17, IFN-γ, TNF-α. Data are shown as mean ± SD. An unpaired t test was performed after the normality test. N = 6 individual donors in each group. (gMFI: Geometric mean fluorescence intensity)

3.3.2.2. Extracellular cytokine secretion after specific stimulation with anti-human CD3 and CD28 antibodies

Although we did not see any apparent differences in intracellular cytokine expression by flow cytometry, we used the multiplex suspension assay to analyze cytokine secretion and its accumulation in the supernatant before (0 h) and 24 h after anti-human CD3 and CD28 stimulation using Transact^{TM}. We observed significantly higher amounts of Transact^{TM} -induced and secreted IL-6, IL-9, interferon γ-induced protein 10kDa (IP-10), monocyte chemotactic and activating factor (MCAF) in the supernatants of memory $CD4^+$ T cells from aged donors in comparison with those examined in young donors (P-values 0.0303, 0.0394, 0.0213, and 0.0152, respectively) (**Figure 3-13**). Furthermore, we observed numerically higher amounts of secreted IFN-γ and TNF-α in the supernatants of memory $CD4^+$ T cells from aged donors when compared to those from young donors.

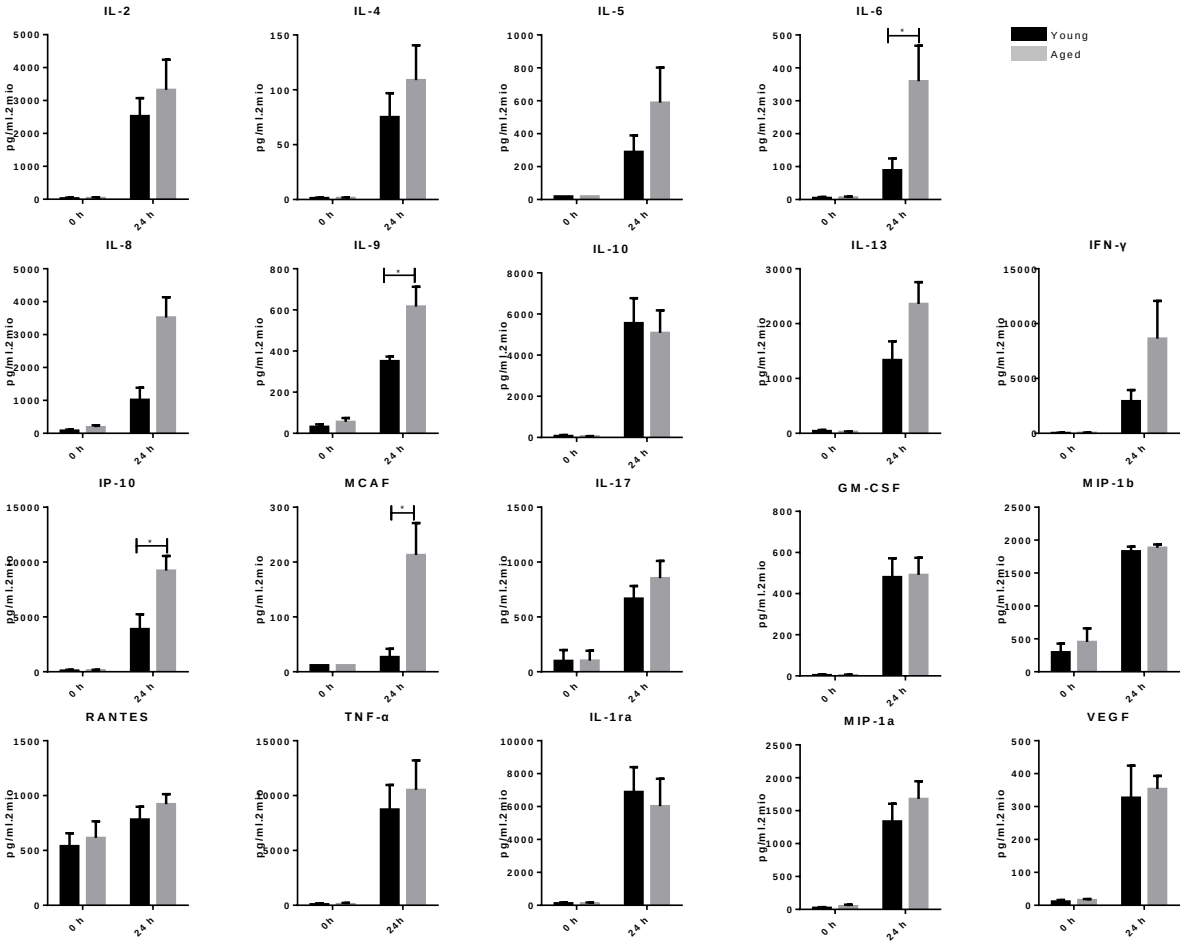

Figure 3-13: Cytokine secretion of memory CD4⁺ T cells in the supernatant. Data from the variety of cytokines showed in this Figure were obtained from the supernatants of memory CD4⁺ T cells of young and aged donors before (0 h) and 24 h after TCR stimulation. Data are shown as mean ± SEM, An unpaired t test was performed after the normality test. Young group: n=5 individual donors, aged group: n=6 individual donors.

4. Discussion

Memory T cells and naive T cells are both quiescent cells, but memory T cells respond much more quickly and robustly to antigens (due to a so-called recall response) than naive cells do, as the latter are supported by a unique metabolic phenotype [57, 58, 59, 60].

In this study, we observed that human memory CD4⁺ T cells had a substantially higher basal respiration when compared to naive CD4⁺ T cells. In studies performed on murine cells, it has been demonstrated that the basal OCR was similar in CD8⁺ memory effector

T (TEM) cells and naive T cells[59]. Conversely, another study demonstrated that $CD8^+$ memory T cells display a higher OCR than naive cells do[57]. In a resting state, memory T cells have been demonstrated to use FAO to generate acetyl-CoA for fueling the TCA cycle and subsequently OxPhos in order to meet their energy demands[58]. However, data from several reports indicate quite a controversial picture of TEM cell metabolism. For instance, although $CD8^+$ memory T cells utilize long-chain FAs for FAO[57], the acquirement of extracellular palmitate (a long-chain FA) is lower in TEMs than in $CD8^+$ effector T cells due to a reduced surface long-chain FA receptor - CD36 expression. Moreover, totally neutral lipids (which indicate stored fat) are significantly reduced, and lipid droplets do not form in $CD8^+$ memory T cells even in the presence of oleate[61, 62]. Furthermore, the amount of OxPhos of $CD8^+$ central memory T (TCM) cells does not increase under FA supplementation conditions. Furthermore, knockout of the two key FA transport proteins – FA binding proteins 4 (FABP4) and 5 (FABP5) – does not affect $CD8^+$ memory T cell survival[63]. All of these data may allow us to suggest that memory T cells consume more FA than they acquire from their external environment. Thus, memory T cells need to utilize a synthesis of FA from the beginning in order to fuel FAO.

Glucose provides an essential carbon source for *de novo* synthesis of FAs. FAs are transferred to ER and stored as triacylglycerol (TAG). TAG is quickly mobilized by lysosomal acid lipase (LAL) to FAs in lysosomes. These FAs are then transferred to the mitochondrial matrix by carnitine palmitoyl transferase 1 (CPT1) and undergo β-oxidation to generate acetyl-CoA which fuels TCA and OxPhos[54, 61]. It is apparent that $CD8^+$ memory T cells engage futile metabolic cycling of *de novo* FA synthesis (FAS) and FAO. The futile cycle is very important for memory cells because it enables memory T cells to engage both glycolysis and OxPhos, to keep biosynthetic processes running, and to provide robust mitochondrial function. All these processes are needed for rapid induction of metabolic reconfiguration through these pathways upon re-encountering an antigen to promote rapid and robust recall responses[58].

In contrast to ‘circulating memory’, tissue-resident memory T (TRM) cells have a metabolic profile that acquires exogenous free FA for FAO to permit long-term survival and function[63]. The totally different source of FA in a TRM subset indicates that the

metabolic phenotype of T memory subsets may in fact be different in specific organs, and this should become a matter of ongoing research.

We also observed that memory $CD4^+$ T cells had a higher percentage of SRC than naive $CD4^+$ T cells do, thereby confirming previous studies which focused on the metabolic profile of $CD8^+$ memory T cells. $CD8^+$ memory T cells have a higher mitochondrial SRC when compared to $CD8^+$ naive T cells[57]. Recently, also human memory $CD4^+$ T cells have been shown to possess an enhanced SRC[60]. Both $CD8^+$ and $CD4^+$ memory T cells have greater mitochondrial masses, supporting an enhanced SRC[57, 60]. Interestingly, when compared to a first immunization, $CD8^+$ T cells after a tertiary immunization have a higher basal OCR and SRC due to a further enlargement of their mitochondrial amount[64]. Therefore, the recall response takes place much more quickly in repetitively-challenged memory T cells.

We found that memory $CD4^+$ T cells have a statistically higher ATP-coupled OCR than naive $CD4^+$ T cells do. Corresponding to our results, human $CD4^+$ TEM cells' ATP coupled-OCR is also higher than that of naive T cells[60]. Higher ATP-coupling was accompanied by higher proton leak in memory $CD4^+$ T cells. Interestingly, memory $CD4^+$ T cells had the same coupling efficiency as naive T cells. However, non-mitochondrial respiration was also higher in memory $CD4^+$ T cells than in naive $CD4^+$ T cells. Research performed using $CD8^+$ T cells showed that there were no differences observed in memory T cells and naive T cells during non-mitochondrial respiration, ATP-coupled OCR, and proton leak[59].

Memory $CD4^+$ T cells had higher basal glycolysis and compensatory glycolysis than naive $CD4^+$ T cells did. In line with our results from the glycolytic assay, human $CD4^+$ TEM cells have a higher basal extracellular acidification rate (ECAR) and glycolytic reserve[60]. In murine $CD8^+$ T cells, one study showed that memory cells had a higher ECAR than naive T cells did[58]; another study showed that TEM had the same basal ECAR, but a higher maximal ECAR than naive T cells[59]. Research on murine $CD8^+$ T cells revealed that $CD8^+$ TEM cells had an enhanced level of cytoplasmic glyceraldehyde-3-phosphate dehydrogenase (GAPDH)[59]. GAPDH is a glycolytic enzyme which is located in the cytoplasm and has a higher activity than the nucleus does[65]. Therefore, cytoplasmic

GAPDH is immediately able to contribute to the increased glycolytic demand under the condition of mitochondrial stress. In support of higher amounts of cytoplasmic GAPDH, $CD8^+$ memory T cells have a higher glycolytic capacity to enable an immediate and early glycolytic switch to recall responses.

Although the research field on immune cell metabolism is well established, its relationship in the field of aging is still relatively new. There are a few studies relating metabolism and T cells to aging in disease models, such as rheumatoid arthritis (RA). Naive CD4 T cells from RA patients reduce glycolytic consumption and have a low lactate production as compared to age-matched donors[66]. The reduced glycolysis is due to insufficient induction of the rate-limiting glycolytic enzyme 6-phosphofructo-2-kinase /fructose-2,6-bisphosphatase 3 (PFKFB3) and overexpression of glucose-6-phosphate dehydrogenase (G6PD)[66, 67]. As a consequence of failing in efficiently inducing aerobic glycolysis (the ‘anti-Warburg-effect’), naive $CD4^+$ T cells from RA patients produce less energy (ATP), undergo apoptosis, display impaired induction of autophagy and shift glucose into the pentose phosphate pathway (PPP). As a result, RA naive T cells generate more nicotinamide adenine dinucleotide phosphate (NADPH), which reduces cellular reactive oxygen species (ROS). ROS reduction shifts naive T cells into pro-inflammatory Th1 or Th17 cells, creating an inflammation-prone T cell pool. In addition, ROS reduction contributes to insufficient activation of the cell cycle kinase and the DNA repair kinase 'ataxia telangiectasia mutated (ATM)'[67]. ATM insufficiency allows RA T cells to skip the G2/M cell cycle checkpoint leading to abnormal proliferation[67] and the repair of DNA inefficiently[68]. Naive $CD4^+$ T cells from RA patients have a low expression of MRE11A which is capable of preparing both single and double-strand break ends for further DNA repair which results in upregulation of senescence markers ($CD57^+$, p16 and p21, etc.). Inhibiting MRE11A activity renders T cell tissue-invasive ability and increases the amounts of pro-inflammatory cytokines' TNF, IL6, and IL1B levels, whereas restoring MRE11A expression in RA T cells reduced infiltration and decreases TNF, IL6, and IL1B expression[69]. DNA repair proteins and a DNA-dependent protein kinase (DNA-PK) also take part in the pathogenic mechanism of RA[70]. An accumulation of damaged DNA is

known to be a vital mechanism in cellular aging[71]. In short, maladaptation of T cell metabolism is linked to an acceleration of cell aging and may to some extent lead to RA. One characteristic of senescent memory T cells is the re-expression of CD45RA. Human $CD8^+$ re-expression of CD45RA memory T cells from 20-35 year-old donors possessed significantly fewer mitochondria, reduced basal OCR and SRC than TEM and TCM did, but revealed a higher glycolysis than TCM did[55]. Recently, a study performed on human classical monocytes demonstrated that aging did reduce mitochondrial maximal respiratory capacity and SRC, but it did not to affect the glycolytic metabolism, and reduced cytokine expression at later time points[72, 73].

However, the actual impact of aging on metabolic phenotype in memory $CD4^+$ T cells still remains unknown today. Here, we first demonstrated that the glycolytic, mitochondrial profile of naive $CD4^+$ T cells and the mitochondrial profile of memory $CD4^+$ T cells did not change during aging; while a decrease of basal glycolysis, compensatory glycolysis, and higher ratio of basal mitoOCR/glycPER of memory $CD4^+$ T cells can be associated with aging. Upon aging, memory $CD4^+$ T cells – in contrast to naive $CD4^+$ T cells – decline in their ability to use glucose, and demonstrate a metabolic phenotype resembling naive $CD4^+$ T cells, in that they may no longer differ between basal glycolysis, compensatory glycolysis and the ratio of basal mitoOCR/glycoPER.

During the process of glycolysis, many intermediates are produced for the generation of fatty acids (FAs), amino acids (AAs) and nucleotides (NTs) as well as for fueling of the pentose phosphate pathway (PPP). We hypothesize from our results that memory $CD4^+$ T cells from aged donors utilize glucose in order to synthesize AAs, FAs, NTs or to fuel PPP instead of being metabolized to lactate. In that way, they facilitate the production of effector molecules and building bricks for cell growth and proliferation. Therefore, we performed functional experiments on memory $CD4^+$ T cells from young and aged donors. As one result, we observed that aging did not affect the proliferation of memory $CD4^+$ T cells. Previously, a study performed in murine $CD8^+$ T cells demonstrated that a lesser percentage of $CD8^+$ T cells from aged mice proliferated due to concanavalin A (Con A) stimulation when compared to the situation in young mice. From these proliferating $CD8^+$ T cells of aged mice, a larger percentage started proliferation later and stopped sooner

than it did in young mice[74]. While focusing on human $CD8^+$ T cells, it has been described that CD45RA-expressing memory T cells (TEMRA cells) demonstrated a decreased proliferation. Moreover, Th1 and Th2 subsets derived from aged mice both decrease in expansion[75]. The differences in the results of these studies and our study may however be due to the different cell types investigated ($CD4^+$ T cells and $CD8^+$ T cells), different characters between human and mice $CD4^+$ T cells, and different accesses utilized to isolate the memory $CD4^+$ T cells (*ex-vivo* or direct).

Inflamm-aging is also mediated by cytokines, such as IL-6, TNF-α, IL-1. We analyzed the intracellular expression of cytokines representing different subsets of $CD4^+$ T cells after 5 h of PMA/Ion stimulation, but found no differences between young and aged donors indicating no differences in Th cell subsets. However, the cytokine expression after T cell activation is a temporal process and follows a specific type of kinetics. Although no differences were observable at the time point of 5 h, the kinetics of cytokine expression in these two groups may, however, still be different. Therefore, we measured the accumulation of cytokine secretion in the supernatant, and found that proinflammatory cytokine (IL-6, IL-9) and chemokine (IP-10, MCAF) were more highly expressed and/or secreted from memory $CD4^+$ T cells of aged donors when compared to those from young donors.

IL-6 is known to be one of the pivotal markers of inflammatory status and a character of aging[76]. Moreover, it is the main cytokine that plays a role in pathophysiological mechanisms involved in age-related diseases[77]. In line with our study, nonagenarians have higher levels of IL-6[76], and in both men and women, increasing age is associated with higher levels of serum IL-6. IL-6 level is also linked to the functional decline in aged individuals, such as poor physical performance and muscle strength[78]. IL-6 is involved in osteoporosis, heart failure, AD, decline in cognitive performance and community-acquired pneumonia requiring hospitalization[79, 80, 81]. A prospective cohort study demonstrated that a high level of IL-6 was also associated with greater mortality[82]. Recently, the role of IL-6 in inflamm-aging was highlighted, inasmuch as an increase of serum IL-6 and the soluble TNF-α receptor-1 were able to predict a 10-year all-cause mortality in older adults[83].

IL-9 is a proinflammatory cytokine which is mainly secreted by Th9 cells. It was first described as a mast cell growth factor, but it also influences immune cells, especially $CD4^+$ T cells. Alongside a well-known role on allergic inflammation and immune response against extracellular parasites, IL-9 plays an important role in infectious diseases[84]. Depletion of IL-9 enhances clearance of respiratory syncytial virus[85], and therefore IL-9 may contribute the declined ability to clear antigens during inflamm-aging. Interestingly, as a classic molecule mediating Th2 responses, IL-9 also plays a role in autoimmune inflammation. Adoptive transfer of *in vitro* polarized Th17 and Th1 induced experimental autoimmune encephalomyelitis (EAE). In line with this, Th9 cells also promoted the generation of EAE upon adoptive transfer, although with different pathological phenotypes[86]. Neutralization of IL-9 as well as IL-9 receptor deficiency alleviated EAE[87, 88]. Conversely, absence of IL-9 signaling aggravated EAE due to its diminishing the suppressive activity of nTregs[89]. The role of IL-9 in autoimmune inflammation – especially during inflamm-aging – needs to be addressed further.

Although senescent T cells tend to produce more TNF-α and IFN-γ[55], we observed no flow cytometric differences in measurements of the intracellular expression of TNF-α and IFN-γ between young and aged groups. However, we did find a numerically higher secretion of TNF-α and IFN-γ from memory $CD4^+$ T cells of aged donors in comparison with those of young donors. A study performed on human activated/memory ($CD95^+CD28^+$) $CD4^+$ T cells showed that the proportions of IFN-γ and TNF-α positive cells decreased significantly during aging[90]. However, the plasma levels of IFN-γ and IL-2 were noted to be unmodified where nonagenarians were compared to young controls[76]. One study showed that memory CD4 T cells generated from aged mice T cells had the same IFN-γ expression in the supernatant when compared to that of young mice, but there was less IL-2, IL-4, and IL-5 expression[75].

Interferon γ-induced protein 10kDa (IP-10), also known as C-X-C motif chemokine 10 (CXCL10), is a member of the CXC chemokine family. IP-10 is also a proinflammatory molecule involved in the leukocyte trafficking and activation of immune cells such as T cells, B cells, macrophages, NK cells, and DCs. The high level of IP-10 in the central nervous system (CNS) is a link to aging-related disease, such as Alzheimer's disease

(AD)[91]. Serum IP-10 significantly increases in age-related macular degeneration (AMD)[92]. The evaluated level of IP-10 expression has also been associated with infectious diseases, autoimmune diseases and tumor development[93, 94].

MCAF has been termed a monocyte chemoattractant protein-1 (MCP-1) belonging to the CC chemokine subfamily. MCAF plays an important role in the recruitment of immune cells, such as monocytes, memory T cells, and DCs, to inflammatory sites[95]. Increased MCAF in synovial fluid of RA recruits mononuclear phagocytes resulting in inflammation associated with RA[96]. Besides autoimmune diseases, MCAF also play a very important role in age-related diseases, such as diabetes, diabetic nephropathy, atherosclerosis, and tumors[95].

In the process of glycolysis, memory $CD4^+$ T cells use more glucose for synthesizing AAs, FAs, NTs or fuel PPP, and this results in the production of effector molecules (**Figure 4-1**). The increase of proinflammatory cytokines (IL-6, IL-9) and chemokines (IP-10, MCAF) of memory $CD4^+$ T cells during aging may contribute to age-related diseases and inflamm-aging.

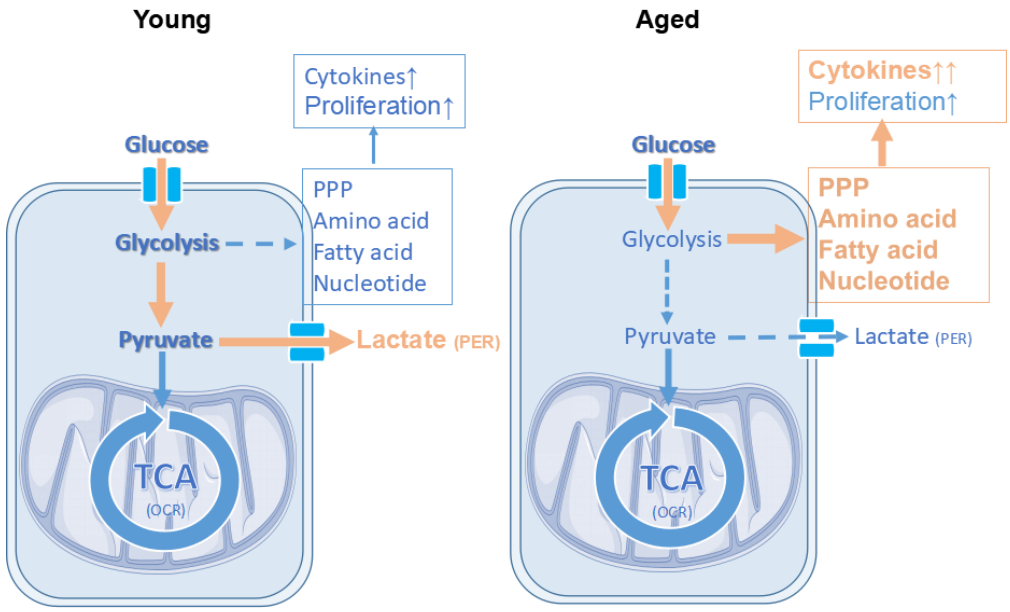

Figure 4-1: Changes of metabolic phenotype and functions in memory $CD4^+$ T cells during aging.

We isolated memory $CD4^+$ T cells by using microbeads based on depletion, and this included CD45RA antibodies. For this, the memory $CD4^+$ T cells we used for the

experiments were without CD45RA re-expression memory $CD4^+$ T cells. That was also confirmed by flow cytometry. CD45RA is one marker of memory T cell senescence[97]. Given this, we used non-senescent memory $CD4^+$ T cells in our experiments. Non-senescent memory $CD4^+$ T cells from aged donors demonstrated different metabolic phenotypes leading to high expression of cytokines, and therefore a metabolic change of memory $CD4^+$ T cells seems to occur earlier than the development of senescent markers does during human aging; non-senescent memory $CD4^+$ T cells during aging also secret a high amount proinflammatory cytokines which may contribute to inflamm-aging.

Although we performed all experiments and the experimental design as precisely as possible, there are still some limitations in this study which remain:

(I) In this study, we divided aged and young groups according to their chronological age and not their biological age. Since there is of course a persistent heterogeneity among age-related diseases of chronologically aged individuals, we thus chose a chronological age variation as large as possible (more than 30 years) in order to show general trends in metabolic and functional differences between aged and young groups.

(II) We measured basal glycolysis according to the proton efflux rate in a Seahorse Analyzer, but did not check directly the glucose consumption and lactate production in resting naive and memory $CD4^+$ T cells from young and aged donors.

(III) We did not measure metabolic differences in naive and memory $CD4^+$ T cells from young and aged donors after stimulation.

(IV) We measured the accumulation of cytokine secretion in supernatants, but did not investigate the kinetics of cytokine expression directly.

(V) Due to data protection issues, we could not compare the body mass index (BMI) in the groups. The first four limitations will be addressed in our further experiments.

In summary, we demonstrated a higher basal glycolysis, basal OCR, and mitochondrial as well as glycolytic capacity of human *ex vivo* memory $CD4^+$ T cells in comparison with that of naive T cells. A decrease of basal glycolysis and compensatory glycolysis in memory $CD4^+$ T cells of aged persons which results in an enhanced expression of proinflammatory cytokines and chemokines can be assumed to culminate in T cell dysfunction leading to the development of inflamm-aging.

References

1. Gallo RL, Nizet V. Innate barriers against skin infection and associated disorders. *Drug Discovery Today: Disease Mechanisms* 2008, **5**(2)**:** e145-e152.

2. Hato T, Dagher PC. How the Innate Immune System Senses Trouble and Causes Trouble. *Clinical journal of the American Society of Nephrology : CJASN* 2015, **10**(8)**:** 1459-1469.

3. Beutler B. Innate immunity: an overview. *Molecular immunology* 2004, **40**(12)**:** 845-859.

4. Medzhitov R, Janeway C, Jr. Innate immunity. *The New England journal of medicine* 2000, **343**(5)**:** 338-344.

5. Flajnik MF, Kasahara M. Origin and evolution of the adaptive immune system: genetic events and selective pressures. *Nature reviews Genetics* 2010, **11**(1)**:** 47-59.

6. Nunez C, Nishimoto N, Gartland GL, Billips LG, Burrows PD, Kubagawa H, Cooper MD. B cells are generated throughout life in humans. *Journal of immunology* 1996, **156**(2)**:** 866-872.

7. Cariappa A, Chase C, Liu H, Russell P, Pillai S. Naive recirculating B cells mature simultaneously in the spleen and bone marrow. *Blood* 2007, **109**(6)**:** 2339-2345.

8. Kruisbeek AM. Introduction: regulation of T cell development by the thymic microenvironment. *Seminars in immunology* 1999, **11**(1)**:** 1-2.

9. Delves PJ, Roitt IM. The immune system. First of two parts. *The New England journal of medicine* 2000, **343**(1)**:** 37-49.

10. Nutt SL, Hodgkin PD, Tarlinton DM, Corcoran LM. The generation of antibody-secreting plasma cells. *Nature reviews Immunology* 2015, **15**(3)**:** 160-171.

11. Barry M, Bleackley RC. Cytotoxic T lymphocytes: all roads lead to death. *Nature reviews Immunology* 2002, **2**(6)**:** 401-409.

12. Sprent J, Surh CD. T cell memory. *Annual review of immunology* 2002, **20:** 551-579.

13. Dutton RW, Bradley LM, Swain SL. T cell memory. *Annual review of immunology* 1998, **16:** 201-223.

14. Rechel B, Grundy E, Robine J-M, Cylus J, Mackenbach JP, Knai C, McKee M. Ageing in the European Union. *The Lancet* 2013, **381**(9874)**:** 1312-1322.

15. Vellas BJ, Albarede JL, Garry PJ. Diseases and aging: patterns of morbidity with age; relationship between aging and age-associated diseases. *The American journal of clinical nutrition* 1992, **55**(6 Suppl)**:** 1225S-1230S.

16. Fontana L. Modulating human aging and age-associated diseases. *Biochimica et biophysica acta* 2009, **1790**(10)**:** 1133-1138.

17. Kennedy BK, Berger SL, Brunet A, Campisi J, Cuervo AM, Epel ES, Franceschi C, Lithgow GJ, Morimoto RI, Pessin JE, Rando TA, Richardson A, Schadt EE, Wyss-Coray T, Sierra F. Geroscience: linking aging to chronic disease. *Cell* 2014, **159**(4)**:** 709-713.

18. Franceschi C, Garagnani P, Parini P, Giuliani C, Santoro A. Inflammaging: a new immune-metabolic viewpoint for age-related diseases. *Nature reviews Endocrinology* 2018, **14**(10)**:** 576-590.

19. Franceschi C, Bonafe M, Valensin S, Olivieri F, De Luca M, Ottaviani E, De Benedictis G. Inflamm-aging. An evolutionary perspective on immunosenescence. *Annals of the New York Academy of Sciences* 2000, **908:** 244-254.

20. Baylis D, Bartlett DB, Patel HP, Roberts HC. Understanding how we age: insights into inflammaging. *Longevity & healthspan* 2013, **2**(1)**:** 8.

21. Agrawal A, Agrawal S, Gupta S. Role of Dendritic Cells in Inflammation and Loss of Tolerance in the Elderly. *Frontiers in immunology* 2017, **8:** 896.

22. Johnston-Carey HK, Pomatto LC, Davies KJ. The Immunoproteasome in oxidative stress, aging, and disease. *Critical reviews in biochemistry and molecular biology* 2015, **51**(4)**:** 268-281.

23. Fulop T, Le Page A, Fortin C, Witkowski JM, Dupuis G, Larbi A. Cellular signaling in the aging immune system. *Current opinion in immunology* 2014, **29:** 105-111.

24. Bryl E, Witkowski JM. Decreased proliferative capability of CD4(+) cells of elderly people is associated with faster loss of activation-related antigens and accumulation of regulatory T cells. *Experimental gerontology* 2004, **39**(4)**:** 587-595.

25. Rider DA, Sinclair AJ, Young SP. Oxidative inactivation of CD45 protein tyrosine phosphatase may contribute to T lymphocyte dysfunction in the elderly. *Mechanisms of ageing and development* 2003, **124**(2)**:** 191-198.

26. Pawelec G. Age and immunity: What is "immunosenescence"? *Experimental gerontology* 2018, **105:** 4-9.

27. Fagnoni FF, Vescovini R, Passeri G, Bologna G, Pedrazzoni M, Lavagetto G, Casti A, Franceschi C, Passeri M, Sansoni P. Shortage of circulating naive CD8(+) T cells provides new insights on immunodeficiency in aging. *Blood* 2000, **95**(9)**:** 2860-2868.

28. Wertheimer AM, Bennett MS, Park B, Uhrlaub JL, Martinez C, Pulko V, Currier NL, Nikolich-Zugich D, Kaye J, Nikolich-Zugich J. Aging and cytomegalovirus infection differentially and jointly affect distinct circulating T cell subsets in humans. *Journal of immunology* 2014, **192**(5)**:** 2143-2155.

29. Qi Q, Liu Y, Cheng Y, Glanville J, Zhang D, Lee JY, Olshen RA, Weyand CM, Boyd SD, Goronzy JJ. Diversity and clonal selection in the human T-cell repertoire. *Proceedings of the National Academy of Sciences of the United States of America* 2014, **111**(36)**:** 13139-13144.

30. den Braber I, Mugwagwa T, Vrisekoop N, Westera L, Mogling R, de Boer AB, Willems N, Schrijver EH, Spierenburg G, Gaiser K, Mul E, Otto SA, Ruiter AF, Ackermans MT, Miedema F, Borghans JA, de Boer RJ, Tesselaar K. Maintenance of peripheral naive T cells is sustained by thymus output in mice but not humans. *Immunity* 2012, **36**(2)**:** 288-297.

31. Fulop T, Larbi A, Dupuis G, Le Page A, Frost EH, Cohen AA, Witkowski JM, Franceschi C. Immunosenescence and Inflamm-Aging As Two Sides of the Same Coin: Friends or Foes? *Frontiers in immunology* 2017, **8:** 1960.

32. Chiu BC, Martin BE, Stolberg VR, Chensue SW. Cutting edge: Central memory CD8 T cells in aged mice are virtual memory cells. *Journal of immunology* 2013, **191**(12)**:** 5793-5796.

33. Nikolich-Zugich J. The twilight of immunity: emerging concepts in aging of the immune system. *Nature immunology* 2018, **19**(1)**:** 10-19.

34. Derhovanessian E, Theeten H, Hahnel K, Van Damme P, Cools N, Pawelec G. Cytomegalovirus-associated accumulation of late-differentiated CD4 T-cells correlates with poor humoral response to influenza vaccination. *Vaccine* 2013, **31**(4)**:** 685-690.

35. Libri V, Azevedo RI, Jackson SE, Di Mitri D, Lachmann R, Fuhrmann S, Vukmanovic-Stejic M, Yong K, Battistini L, Kern F, Soares MV, Akbar AN. Cytomegalovirus infection induces the accumulation of short-lived, multifunctional CD4+CD45RA+CD27+ T cells: the potential involvement of interleukin-7 in this

process. *Immunology* 2011, **132**(3)**:** 326-339.

36. Akbar AN, Henson SM, Lanna A. Senescence of T Lymphocytes: Implications for Enhancing Human Immunity. *Trends in immunology* 2016, **37**(12)**:** 866-876.

37. Goronzy JJ, Weyand CM. Immune aging and autoimmunity. *Cellular and molecular life sciences : CMLS* 2012, **69**(10)**:** 1615-1623.

38. Lages CS, Suffia I, Velilla PA, Huang B, Warshaw G, Hildeman DA, Belkaid Y, Chougnet C. Functional regulatory T cells accumulate in aged hosts and promote chronic infectious disease reactivation. *Journal of immunology* 2008, **181**(3)**:** 1835-1848.

39. van der Geest KS, Abdulahad WH, Tete SM, Lorencetti PG, Horst G, Bos NA, Kroesen BJ, Brouwer E, Boots AM. Aging disturbs the balance between effector and regulatory CD4+ T cells. *Experimental gerontology* 2014, **60:** 190-196.

40. Gaber T, Strehl C, Buttgereit F. Metabolic regulation of inflammation. *Nature reviews Rheumatology* 2017, **13**(5)**:** 267-279.

41. O'Neill LA, Kishton RJ, Rathmell J. A guide to immunometabolism for immunologists. *Nature reviews Immunology* 2016, **16**(9)**:** 553-565.

42. Donnelly RP, Finlay DK. Glucose, glycolysis and lymphocyte responses. *Molecular immunology* 2015, **68**(2 Pt C)**:** 513-519.

43. Gaber T, Chen Y, Krauss PL, Buttgereit F. Metabolism of T Lymphocytes in Health and Disease. *International review of cell and molecular biology* 2019, **342:** 95-148.

44. Warburg O, Gawehn K, Geissler AW. [Metabolism of leukocytes]. *Zeitschrift fur Naturforschung Teil B, Chemie, Biochemie, Biophysik, Biologie und verwandte Gebiete* 1958, **13B**(8)**:** 515-516.

45. Warburg O, Gawehn K, Geissler AW. [The transformation of embryonal metabolism in cancer metabolism]. *Zeitschrift fur Naturforschung Teil B, Chemie, Biochemie, Biophysik, Biologie und verwandte Gebiete* 1960, **15B:** 378-379.

46. Loftus RM, Finlay DK. Immunometabolism: Cellular Metabolism Turns Immune Regulator. *The Journal of biological chemistry* 2016, **291**(1)**:** 1-10.

47. Mehta MM, Weinberg SE, Chandel NS. Mitochondrial control of immunity: beyond ATP. *Nature reviews Immunology* 2017, **17**(10)**:** 608-620.

48. Ghesquiere B, Wong BW, Kuchnio A, Carmeliet P. Metabolism of stromal and

immune cells in health and disease. *Nature* 2014, **511**(7508)**:** 167-176.

49. Bantug GR, Galluzzi L, Kroemer G, Hess C. The spectrum of T cell metabolism in health and disease. *Nature reviews Immunology* 2018, **18**(1)**:** 19-34.

50. MacIver NJ, Michalek RD, Rathmell JC. Metabolic regulation of T lymphocytes. *Annual review of immunology* 2013, **31:** 259-283.

51. Macintyre AN, Gerriets VA, Nichols AG, Michalek RD, Rudolph MC, Deoliveira D, Anderson SM, Abel ED, Chen BJ, Hale LP, Rathmell JC. The glucose transporter Glut1 is selectively essential for CD4 T cell activation and effector function. *Cell metabolism* 2014, **20**(1)**:** 61-72.

52. Chang CH, Curtis JD, Maggi LB, Jr., Faubert B, Villarino AV, O'Sullivan D, Huang SC, van der Windt GJ, Blagih J, Qiu J, Weber JD, Pearce EJ, Jones RG, Pearce EL. Posttranscriptional control of T cell effector function by aerobic glycolysis. *Cell* 2013, **153**(6)**:** 1239-1251.

53. Sena LA, Li S, Jairaman A, Prakriya M, Ezponda T, Hildeman DA, Wang CR, Schumacker PT, Licht JD, Perlman H, Bryce PJ, Chandel NS. Mitochondria are required for antigen-specific T cell activation through reactive oxygen species signaling. *Immunity* 2013, **38**(2)**:** 225-236.

54. Cui G, Staron MM, Gray SM, Ho PC, Amezquita RA, Wu J, Kaech SM. IL-7-Induced Glycerol Transport and TAG Synthesis Promotes Memory CD8+ T Cell Longevity. *Cell* 2015, **161**(4)**:** 750-761.

55. Henson SM, Lanna A, Riddell NE, Franzese O, Macaulay R, Griffiths SJ, Puleston DJ, Watson AS, Simon AK, Tooze SA, Akbar AN. p38 signaling inhibits mTORC1-independent autophagy in senescent human CD8(+) T cells. *The Journal of clinical investigation* 2014, **124**(9)**:** 4004-4016.

56. Yu M, Li G, Lee WW, Yuan M, Cui D, Weyand CM, Goronzy JJ. Signal inhibition by the dual-specific phosphatase 4 impairs T cell-dependent B-cell responses with age. *Proceedings of the National Academy of Sciences of the United States of America* 2012, **109**(15)**:** E879-888.

57. van der Windt GJ, Everts B, Chang CH, Curtis JD, Freitas TC, Amiel E, Pearce EJ, Pearce EL. Mitochondrial respiratory capacity is a critical regulator of CD8+ T cell memory development. *Immunity* 2012, **36**(1)**:** 68-78.

58. van der Windt GJ, O'Sullivan D, Everts B, Huang SC, Buck MD, Curtis JD, Chang CH, Smith AM, Ai T, Faubert B, Jones RG, Pearce EJ, Pearce EL. CD8 memory T cells have a bioenergetic advantage that underlies their rapid recall ability.

Proceedings of the National Academy of Sciences of the United States of America 2013, **110**(35)**:** 14336-14341.

59. Gubser PM, Bantug GR, Razik L, Fischer M, Dimeloe S, Hoenger G, Durovic B, Jauch A, Hess C. Rapid effector function of memory CD8+ T cells requires an immediate-early glycolytic switch. *Nature immunology* 2013, **14**(10)**:** 1064-1072.

60. Dimeloe S, Mehling M, Frick C, Loeliger J, Bantug GR, Sauder U, Fischer M, Belle R, Develioglu L, Tay S, Langenkamp A, Hess C. The Immune-Metabolic Basis of Effector Memory CD4+ T Cell Function under Hypoxic Conditions. *Journal of immunology* 2016, **196**(1)**:** 106-114.

61. O'Sullivan D, van der Windt GJ, Huang SC, Curtis JD, Chang CH, Buck MD, Qiu J, Smith AM, Lam WY, DiPlato LM, Hsu FF, Birnbaum MJ, Pearce EJ, Pearce EL. Memory CD8(+) T cells use cell-intrinsic lipolysis to support the metabolic programming necessary for development. *Immunity* 2014, **41**(1)**:** 75-88.

62. Silverstein RL, Febbraio M. CD36, a scavenger receptor involved in immunity, metabolism, angiogenesis, and behavior. *Science signaling* 2009, **2**(72)**:** re3.

63. Pan Y, Tian T, Park CO, Lofftus SY, Mei S, Liu X, Luo C, O'Malley JT, Gehad A, Teague JE, Divito SJ, Fuhlbrigge R, Puigserver P, Krueger JG, Hotamisligil GS, Clark RA, Kupper TS. Survival of tissue-resident memory T cells requires exogenous lipid uptake and metabolism. *Nature* 2017, **543**(7644)**:** 252-256.

64. Fraser KA, Schenkel JM, Jameson SC, Vezys V, Masopust D. Preexisting high frequencies of memory CD8+ T cells favor rapid memory differentiation and preservation of proliferative potential upon boosting. *Immunity* 2013, **39**(1)**:** 171-183.

65. Mazzola JL, Sirover MA. Subcellular localization of human glyceraldehyde-3-phosphate dehydrogenase is independent of its glycolytic function. *Biochimica et biophysica acta* 2003, **1622**(1)**:** 50-56.

66. Yang Z, Fujii H, Mohan SV, Goronzy JJ, Weyand CM. Phosphofructokinase deficiency impairs ATP generation, autophagy, and redox balance in rheumatoid arthritis T cells. *The Journal of experimental medicine* 2013, **210**(10)**:** 2119-2134.

67. Yang Z, Shen Y, Oishi H, Matteson EL, Tian L, Goronzy JJ, Weyand CM. Restoring oxidant signaling suppresses proarthritogenic T cell effector functions in rheumatoid arthritis. *Science translational medicine* 2016, **8**(331)**:** 331ra338.

68. Shao L, Fujii H, Colmegna I, Oishi H, Goronzy JJ, Weyand CM. Deficiency of the DNA repair enzyme ATM in rheumatoid arthritis. *The Journal of experimental*

medicine 2009, **206**(6)**:** 1435-1449.

69. Li Y, Shen Y, Hohensinner P, Ju J, Wen Z, Goodman SB, Zhang H, Goronzy JJ, Weyand CM. Deficient Activity of the Nuclease MRE11A Induces T Cell Aging and Promotes Arthritogenic Effector Functions in Patients with Rheumatoid Arthritis. *Immunity* 2016, **45**(4)**:** 903-916.

70. Shao L, Goronzy JJ, Weyand CM. DNA-dependent protein kinase catalytic subunit mediates T-cell loss in rheumatoid arthritis. *EMBO molecular medicine* 2010, **2**(10)**:** 415-427.

71. Li Y, Goronzy JJ, Weyand CM. DNA damage, metabolism and aging in pro-inflammatory T cells: Rheumatoid arthritis as a model system. *Experimental gerontology* 2018, **105:** 118-127.

72. Pence BD, Yarbro JR. Aging impairs mitochondrial respiratory capacity in classical monocytes. *Experimental gerontology* 2018, **108:** 112-117.

73. Pence BD, Yarbro JR. Classical monocytes maintain ex vivo glycolytic metabolism and early but not later inflammatory responses in older adults. *Immunity & ageing : I & A* 2019, **16:** 3.

74. Jiang J, Gross D, Elbaum P, Murasko DM. Aging affects initiation and continuation of T cell proliferation. *Mechanisms of ageing and development* 2007, **128**(4)**:** 332-339.

75. Haynes L, Eaton SM, Burns EM, Randall TD, Swain SL. CD4 T cell memory derived from young naive cells functions well into old age, but memory generated from aged naive cells functions poorly. *Proceedings of the National Academy of Sciences of the United States of America* 2003, **100**(25)**:** 15053-15058.

76. Palmeri M, Misiano G, Malaguarnera M, Forte GI, Vaccarino L, Milano S, Scola L, Caruso C, Motta M, Maugeri D, Lio D. Cytokine serum profile in a group of Sicilian nonagenarians. *Journal of immunoassay & immunochemistry* 2012, **33**(1)**:** 82-90.

77. Maggio M, Guralnik JM, Longo DL, Ferrucci L. Interleukin-6 in aging and chronic disease: a magnificent pathway. *The journals of gerontology Series A, Biological sciences and medical sciences* 2006, **61**(6)**:** 575-584.

78. Cesari M, Penninx BW, Pahor M, Lauretani F, Corsi AM, Rhys Williams G, Guralnik JM, Ferrucci L. Inflammatory markers and physical performance in older persons: the InCHIANTI study. *The journals of gerontology Series A, Biological sciences and medical sciences* 2004, **59**(3)**:** 242-248.

79. Michaud M, Balardy L, Moulis G, Gaudin C, Peyrot C, Vellas B, Cesari M, Nourhashemi F. Proinflammatory cytokines, aging, and age-related diseases. *Journal of the American Medical Directors Association* 2013, **14**(12)**:** 877-882.

80. Minciullo PL, Catalano A, Mandraffino G, Casciaro M, Crucitti A, Maltese G, Morabito N, Lasco A, Gangemi S, Basile G. Inflammaging and Anti-Inflammaging: The Role of Cytokines in Extreme Longevity. *Archivum immunologiae et therapiae experimentalis* 2016, **64**(2)**:** 111-126.

81. Yende S, Tuomanen EI, Wunderink R, Kanaya A, Newman AB, Harris T, de Rekeneire N, Kritchevsky SB. Preinfection systemic inflammatory markers and risk of hospitalization due to pneumonia. *American journal of respiratory and critical care medicine* 2005, **172**(11)**:** 1440-1446.

82. Giovannini S, Onder G, Liperoti R, Russo A, Carter C, Capoluongo E, Pahor M, Bernabei R, Landi F. Interleukin-6, C-reactive protein, and tumor necrosis factor-alpha as predictors of mortality in frail, community-living elderly individuals. *Journal of the American Geriatrics Society* 2011, **59**(9)**:** 1679-1685.

83. Varadhan R, Yao W, Matteini A, Beamer BA, Xue QL, Yang H, Manwani B, Reiner A, Jenny N, Parekh N, Fallin MD, Newman A, Bandeen-Roche K, Tracy R, Ferrucci L, Walston J. Simple biologically informed inflammatory index of two serum cytokines predicts 10 year all-cause mortality in older adults. *The journals of gerontology Series A, Biological sciences and medical sciences* 2014, **69**(2)**:** 165-173.

84. Goswami R, Kaplan MH. A brief history of IL-9. *Journal of immunology* 2011, **186**(6)**:** 3283-3288.

85. Dodd JS, Lum E, Goulding J, Muir R, Van Snick J, Openshaw PJ. IL-9 regulates pathology during primary and memory responses to respiratory syncytial virus infection. *Journal of immunology* 2009, **183**(11)**:** 7006-7013.

86. Jager A, Dardalhon V, Sobel RA, Bettelli E, Kuchroo VK. Th1, Th17, and Th9 effector cells induce experimental autoimmune encephalomyelitis with different pathological phenotypes. *Journal of immunology* 2009, **183**(11)**:** 7169-7177.

87. Li H, Nourbakhsh B, Ciric B, Zhang GX, Rostami A. Neutralization of IL-9 ameliorates experimental autoimmune encephalomyelitis by decreasing the effector T cell population. *Journal of immunology* 2010, **185**(7)**:** 4095-4100.

88. Nowak EC, Weaver CT, Turner H, Begum-Haque S, Becher B, Schreiner B, Coyle AJ, Kasper LH, Noelle RJ. IL-9 as a mediator of Th17-driven inflammatory disease. *The Journal of experimental medicine* 2009, **206**(8)**:** 1653-1660.

89. Elyaman W, Bradshaw EM, Uyttenhove C, Dardalhon V, Awasthi A, Imitola J, Bettelli E, Oukka M, van Snick J, Renauld JC, Kuchroo VK, Khoury SJ. IL-9 induces differentiation of TH17 cells and enhances function of FoxP3+ natural regulatory T cells. *Proceedings of the National Academy of Sciences of the United States of America* 2009, **106**(31)**:** 12885-12890.

90. Alberti S, Cevenini E, Ostan R, Capri M, Salvioli S, Bucci L, Ginaldi L, De Martinis M, Franceschi C, Monti D. Age-dependent modifications of Type 1 and Type 2 cytokines within virgin and memory CD4+ T cells in humans. *Mechanisms of ageing and development* 2006, **127**(6)**:** 560-566.

91. Vinet J, de Jong EK, Boddeke HW, Stanulovic V, Brouwer N, Granic I, Eisel UL, Liem RS, Biber K. Expression of CXCL10 in cultured cortical neurons. *Journal of neurochemistry* 2010, **112**(3)**:** 703-714.

92. Mo FM, Proia AD, Johnson WH, Cyr D, Lashkari K. Interferon gamma-inducible protein-10 (IP-10) and eotaxin as biomarkers in age-related macular degeneration. *Investigative ophthalmology & visual science* 2010, **51**(8)**:** 4226-4236.

93. Liu M, Guo S, Hibbert JM, Jain V, Singh N, Wilson NO, Stiles JK. CXCL10/IP-10 in infectious diseases pathogenesis and potential therapeutic implications. *Cytokine & growth factor reviews* 2011, **22**(3)**:** 121-130.

94. Liu M, Guo S, Stiles JK. The emerging role of CXCL10 in cancer (Review). *Oncology letters* 2011, **2**(4)**:** 583-589.

95. Yadav A, Saini V, Arora S. MCP-1: chemoattractant with a role beyond immunity: a review. *Clinica chimica acta; international journal of clinical chemistry* 2010, **411**(21-22)**:** 1570-1579.

96. Koch AE, Kunkel SL, Harlow LA, Johnson B, Evanoff HL, Haines GK, Burdick MD, Pope RM, Strieter RM. Enhanced production of monocyte chemoattractant protein-1 in rheumatoid arthritis. *The Journal of clinical investigation* 1992, **90**(3)**:** 772-779.

97. Xu W, Larbi A. Markers of T Cell Senescence in Humans. *International journal of molecular sciences* 2017, **18**(8).

Eidesstattliche Versicherung

„Ich, Yuling Chen, versichere an Eides statt durch meine eigenhändige Unterschrift, dass ich die vorgelegte Dissertation mit dem Thema: „*Immunometabolism of inflamm-aging in naive and memory CD4⁺ T cells.*“ selbstständig und ohne nicht offengelegte Hilfe Dritter verfasst und keine anderen als die angegebenen Quellen und Hilfsmittel genutzt habe. Alle Stellen, die wörtlich oder dem Sinne nach auf Publikationen oder Vorträgen anderer Autoren beruhen, sind als solche in korrekter Zitierung kenntlich gemacht. Die Abschnitte zu Methodik (insbesondere praktische Arbeiten, Laborbestimmungen, statistische Aufarbeitung) und Resultaten (insbesondere Abbildungen, Graphiken und Tabellen werden von mir verantwortet.

Meine Anteile an etwaigen Publikationen zu dieser Dissertation entsprechen denen, die in der untenstehenden gemeinsamen Erklärung mit dem/der Betreuer/in, angegeben sind. Für sämtliche im Rahmen der Dissertation entstandenen Publikationen wurden die Richtlinien des ICMJE (International Committee of Medical Journal Editors; www.icmje.og) zur Autorenschaft eingehalten. Ich erkläre ferner, dass mir die Satzung der Charité – Universitätsmedizin Berlin zur Sicherung Guter Wissenschaftlicher Praxis bekannt ist und ich mich zur Einhaltung dieser Satzung verpflichte.

Die Bedeutung dieser eidesstattlichen Versicherung und die strafrechtlichen Folgen einer unwahren eidesstattlichen Versicherung (§156,161 des Strafgesetzbuches) sind mir bekannt und bewusst.“

Datum Unterschrift

Curriculum Vitae

For reasons of data protection, my CV will not be published in the electronic version of my work.

List of publications

Publication

Gaber T, **Chen Y,** Krauß PL , Buttgereit F. Metabolism of T Lymphocytes in Health and Disease. Int Rev Cell Mol Biol. 2019; 342:95-148.

Presentation

Chen Y: Metabolism of inflamm-aging in naive and memory $CD4^+$ T helper cells. In: Department of Gastroenterology, Infectiology and Rheumatology, Charite: 26.02.2019 Berlin; 2019.

Poster

Chen Y, Löwe P, Wu H, Buttgereit F, Gaber T: Metabolic changes of human ex vivo naive and memory $CD4^+$ T cells during aging. DGRh, Mannheim;2018.

Acknowledgements

First, I am very grateful to Professor Frank Buttgereit for offering the precious opportunity to do research work in his group, for guiding my biogenetical research on the immune system, and for his great support.
I would like to express my endless gratitude to Timo Gaber for his supervision of my scientific research practice, for sincere encouragement, dedicated support, constructive advice, and for his patience. Without his specialist knowledge, my doctoral thesis would not have been possible.
I truly appreciate all of my colleagues in Professor Buttgereit's working group for the friendly atmosphere. I thank Cindy Strehl for her constant helpfulness and suggestions during my research, and many thanks to Manuela Jakstadt for performing the multiplex suspension assay (Bio-Plex) and ordering reagents. I would like to thank Dimas Abdirama for the help in cell isolation and flow cytometry. I thank Pierre-Louis Krauß for suggestions especially at the beginning of my research. Special thanks are delivered to Moritz Pfeiffenberger for his support, not only in research but also in daily life such as securing a place in a kindergarden for my daughter and moving from apartment to apartment. I thank Annemarie Lang for documental working. Many thanks to Alexandra Damerau, Lisa Ehlers, Pelle Löwe, Siska Wilantri, Franziska Heinsohn, Marie-Christin Weber, Justyna Pienczykowski, Antonia Clara Katharina, and Aditi Kuppe.
Special thanks also go to Dr. Rainer Glauben, Dr. Hao Wu in the group of Siegmund for providing Seahorse Technology and for the opportunity to join their lab meetings to present my data and to gain fruitful discussion and constructive suggestions.
I would like to thank all donors who have donated their blood and filters for my research.
I also sincerely thank all of my friends in Berlin. With all of you, I had such a wonderful time here in the past 3 years. Thanks are also due to the Scholarship Council (CSC) for financial support during my research.
Last but not least, I want to thank my family. I thank my father and mother, and father-in-law and mother-in-law for your great love, endless support and understanding. I thank my brother for your great support, and I always wish you all the best, I thank you, my husband, Yuanchun Ye, for your support in all circumstances. I thank you – Yiyi, my little honey – for your company, I love you so much.